Composite Structures 321 (2023) 117225

Contents lists available at ScienceDirect

Composite Structures

journal homepage: www.elsevier.com/locate/compstruct

On the size-dependent electro-mechanical response of the piezoelectric microbeam

Guangyang Fu [a], Zhenjie Zhang [c], Chunmei Dong [a], Guangxi Zhao [a], Jianjun Wang [a,*], Xuye Zhuang [a,b,*], Hongyu Zheng [a,*]

[a] Centre for Advanced Laser Manufacturing (CALM), School of Mechanical Engineering, Shandong University of Technology, Zibo, Shandong 255000, People's Republic of China

[b] State Key Laboratory of Applied Optics, Changchun Institute of Optics, Fine Mechanics and Physics, Chinese Academy of Sciences, Changchun, Jilin 130033, People's Republic of China

[c] School of Mechanical Engineering, Shandong University, Jinan, Shandong 250061, People's Republic of China

ARTICLE INFO

Keywords:
Size effects
Electro-mechanical response
Strain gradient effects
Flexoelectric effects
Piezoelectric effects

ABSTRACT

Classical piezoelectric elasticity theory fails to explain the size-dependent electro-mechanical behaviour. The strain gradient elasticity and flexoelectricity are responsible for the size effects phenomenon. In this paper, the general strain gradient elasticity is incorporated into the flexoelectric elasticity theory to describe the size dependency. The degeneration analysis of the flexoelectric elasticity theory incorporating the general strain gradient elasticity is performed. The flexoelectric elasticity theory incorporating the general strain gradient elasticity includes all strain gradients, and can degenerate to the simplified flexoelectric elasticity theories incorporating the approximated strain gradient elasticity when some strain gradients are ignored. Subsequently, the differences between the general theory and the simplified theories in describing the size effects are revealed by solving the direct/inverse electro-mechanical problems of the laminated microbeam with a partially covered piezoelectric layer under the uniformly distributed load and external voltage. Compared with the general theory, the simplified theories predict larger collected charge, polarization, electric potential and deflection, and thus underestimate the size-dependent electro-mechanical response. Moreover, the contributions from the strain gradient elasticity and flexoelectricity to the electro-mechanical behaviour are further identified, respectively. The strain gradient elasticity consideration significantly weakens the flexoelectricity and piezoelectricity when the beam thickness is comparable to the material length-scale parameters. The flexoelectricity enhances the polarization, weakens the electric potential while hardly affects the deflection when the beam thickness is in micron range.

1. Introduction

The electro-mechanical responses of the piezoelectric microcomponents show size dependency [1–3]. The strain gradient elasticity and flexoelectricity contribute to the size-dependent electro-mechanical response. Classical piezoelectric elasticity theory without these factors fails to explain the size effects phenomenon [4]. Therefore, the extended piezoelectric elasticity theory including the piezoelectric strain gradient elasticity theory and the flexoelectric elasticity theory is developed to describe the size dependency.

For the piezoelectric strain gradient elasticity theory, the strain gradient elasticity is incorporated to describe the strain gradient effects. According to the incorporated strain gradient elasticity, the piezoelectric strain gradient elasticity theories generally include the piezoelectric classical couple stress theory and the piezoelectric strain gradient elasticity theory. The piezoelectric classical couple stress theory [5] originates from the classical couple stress theory [6,7] and considers the rotational gradients to be equivalent to the strain gradients. Subsequently, based on the understanding of the contribution from the rotational gradient component to the size effects [8,9], the piezoelectric classical couple stress theory was modified to be the piezoelectric symmetric couple stress theory [10] and the piezoelectric anti-symmetric couple stress theory [11], respectively. The piezoelectric symmetric couple stress theory considers the symmetric rotational gradient component individually contribute to the size effects while the piezoelectric anti-symmetric couple stress theory uses the anti-symmetric rotational gradient component as an alternative. The perspective about the contribution from the symmetric/anti-symmetric rotational gradient component to the size effects is obviously contradict. Münch et al. [12]

* Corresponding authors.
E-mail addresses: kai0827@163.com (J. Wang), zhenghongyu@sdut.edu.cn (H. Zheng).

https://doi.org/10.1016/j.compstruct.2023.117225
Received 13 October 2022; Received in revised form 2 May 2023; Accepted 1 June 2023
Available online 12 June 2023

and Neff et al. [13] together explored the essential reason behind the contradiction, and concluded that the symmetric/anti-symmetric rotational gradient component actually contributes to the size effects simultaneously. The similar conclusion was also presented by Shaat [14] and Fu et al. [15], respectively. However, the rotational gradients belongs to the anti-symmetric part of the strain gradients [16]. Thus, the piezoelectric classical couple stress theory and the modified versions underestimate the strain gradient effects.

To include all strain gradients, Mindlin [17] proposed the original strain gradient elasticity theory with five material length-scale parameters. The original strain gradient elasticity theory contains too many material length-scale parameters to apply conveniently. For convenient application, Lam et al. [18] modified the original strain gradient elasticity theory by introducing the constraint of the moments of couples. Subsequently, the modified strain gradient elasticity was incorporated into the classical piezoelectric elasticity theory to describe the size dependency [19]. However, the rationality of introduction of the constraint of the moments of couples is worthy of discussion due to the free character of moment vectors [12]. Based on the orthogonal decomposition of the strain gradient tensor, Zhou et al. [20] demonstrated the number of independent higher-order material parameters for the isotropic material is three, reformulated the original strain gradient elasticity theory [17] and established the general strain gradient elasticity theory with three independent material length-scale parameters. By ignoring part of strain gradients, the simplified strain gradient elasticity theory with only one material length-scale parameter was proposed [21,22] and further extended to the piezoelectric material [23]. The simplified strain gradient elasticity theory with one material length-scale parameter fails to deal with the size effects phenomenon effectively [24,25].

Besides the piezoelectric strain gradient elasticity theory, the flexoelectric elasticity theory is also proposed to explain the electro-mechanical response of the piezoelectric microstructures. The flexoelectric elasticity theory initially focused on the direct/inverse flexoelectric effects. Mindlin [26] extended the classical piezoelectric elasticity theory to include the polarization gradients. Tagantsev [27] combined the phenomenological and microscopic method to demonstrate that the static or dynamic bulk/surface flexoelectric effects are the main influential mechanism of flexoelectricity. Yan and Jiang [28] paid attention to the direct flexoelectric effects and polarization effects. Huang et al. [29] focused on the inverse flexoelectric effects. Barati [30] further considered the polarization gradient effects. Majdoub et al. [31] simplified the original flexoelectric elasticity theory [32] by neglecting the higher-order terms, and proposed the flexoelectric elasticity theory with direct/inverse flexoelectric effects, polarization effects, polarization gradient effects and piezoelectric effects.

The above flexoelectric elasticity theories neglected the strain gradient elasticity while the strain gradient effects is significant at small scale [33]. Therefore, Emad et al. [34] considered the strain gradient effects and direct flexoelectric effects. The original strain gradient elasticity theory [17] is used to describe the strain gradient effects. The strain and strain gradient coupling effects is also studied [35,36]. Li and Luo [37] further considered the strain gradient effects and direct/inverse flexoelectric effects. However, the symmetric couple stress theory [8] is applied to explain the strain gradient effects, and underestimates the size effects. Wang and Wang [38] neglected the axial strain gradient effects for simplicity. Sahin and Dost [32] comprehensively considered the first and second gradients of the displacement, and subsequently developed the original theoretical framework of the flexoelectricity. However, the complicated form of the original theory leads to the constraint of practical application. Subsequently, Hu and Shen [39] established the general flexoelectric elasticity theory with the strain gradient effects, polarization effects, polarization gradient effects and the flexoelectric effects. The surface effects including the surface stress effects and surface polarization effects was further considered [40].

Based on the flexoelectric elasticity theory, the electro-mechanical analysis of the piezoelectric microstructures is performed. For the piezoelectric microbeam, Zhang and Li [41] and Zhou et al. [42] respectively solved the bending problem of the piezoelectric microbeams with flexoelectric effects. Subsequently, this solution was extended to the functionally graded piezoelectric material [43]. Su et al. [44] further solved the bending problem of the bilayer microbeam. Fu et al. [45] extended the solution to the laminated microbeam with a partially covered flexoelectric layer. The vibration analysis of the piezoelectric microbeam was respectively performed by Li and Luo [37] and Chen et al. [46]. Sondipon [47] and Malikan and Eremeyev [48] considered the effects from the viscoelastic medium and the porosity, respectively. Wang and Wang [49] performed the vibration analysis of the bilayer microbeam with piezoelectricity and flexoelectricity. The influences from the nonlinearity and surface properties were also considered [50]. Liang et al. [51] further solved the vibration problem of three-layered piezoelectric microbeam. Yan and Jiang [28] comprehensively explored the bending and vibration responses. The corresponding nonlinear analysis was subsequently performed [52]. Ghobadi et al. [53] further considered the magnetic effects. Jankowski et al. [54] performed the buckling analysis of the piezoelectric microbeam. The extension problem of the piezoelectric bar considering the strain gradient elasticity and flexoelectricity was also solved [55]. For the piezoelectric microplate, Yan [56] performed the static analysis of the piezoelectric microplate with various boundary conditions. The nonlinear bending problem was subsequently solved [57]. Zhang et al. [58] and Yan et al. [59] further derived the bending and vibration solutions of the circular microplate with flexoelectricity, respectively. The influences of the strain gradient elasticity, flexoelectricity and piezoelectricity on the dynamic performance of the bilayer circular microplate were also studied [60]. Guinovart-Sanjuán et al. [61] applied the asymptotic homogenization method to derive the close-form solutions for the effective properties of a two-layer laminate composite with cubic crystal symmetry constituents and perfect contact at the interface. Subsequently, the similar method was extended to illustrate the behaviour of effective properties for bi-materials rectangular and wavy laminated composites [62]. To include the contributions from the imperfect interface conditions, Serpilli et al. [63] developed a new imperfect interface contact approach in flexoelectricity based on the asymptotic analysis, solved the equilibrium problem of a flexoelectric three-layer micro-bar, and discussed the nonlocal phenomena and end-effects associated with the flexoelectric length-scale parameter. The development of the electro-mechanical models of piezoelectric microstructures was further reviewed [64,65].

According to above analysis, the research about the combined effects of strain gradient elasticity and flexoelectricity on the electro-mechanical response of the piezoelectric microcomponents becomes the focus. The focus can be concluded as two aspects: one is the theoretical study of extended piezoelectric elasticity theory, and the other is the model study of advanced composite structures. For the theoretical study, compared with the flexoelectric effects that the expression is explicit, various strain gradient elasticity is incorporated to describe the strain gradient effects. However, the influential mechanism of different strain gradient elasticity on the electro-mechanical response of piezoelectric microcomponents is still unclear. For the model study, the piezoelectric microcomponents including the monolayer or bilayer microbeam/microplate are the main research interests. Compared with the monolayer or bilayer piezoelectric structure, the laminated structure with a partially cover piezoelectric layer is a more general structural form. As the key microcomponents of many classical micro-devices, the electro-mechanical model of the laminated microbeam with a partially cover piezoelectric layer has not been established. Therefore, this paper devoted to theoretically clarify the relations among different strain gradient elasticity, establish the size-dependent electro-mechanical model of the laminated microbeam with

a partially cover piezoelectric layer, and identify the influential mechanism of different strain gradient elasticity on the electro-mechanical response of the partially coved laminated piezoelectric microbeam.

In this paper, the general strain gradient elasticity [20] with three independent material length-scale parameters is incorporated into the flexoelectric elasticity theory to perform the size-dependent electro-mechanical analysis of the piezoelectric microstructures. The degeneration of the flexoelectric elasticity theory incorporating the general strain gradient elasticity is discussed. Subsequently, the ability of the flexoelectric elasticity theory incorporating the general strain gradient elasticity or the approximated strain gradient elasticity in describing the size-dependent electro-mechanical response is compared by performing the bending analysis of the laminated microbeam with a partially covered piezoelectric layer under the uniformly distributed load and external voltage. The direct/inverse electro-mechanical problems are solved. The size-dependent electro-mechanical responses are studied, and the contributions from the strain gradient elasticity and flexoelectricity to the electro-mechanical behaviour are further identified, respectively.

The paper is organized as follows. In Section 2, we reviewed the basic theoretical equations of the flexoelectric elasticity theory with the general strain gradient elasticity. Subsequently, the degeneration of the flexoelectric elasticity theory with the general strain gradient elasticity is discussed. Then, in Section 3, we derived the boundary conditions and governing equations of the laminated microbeam with a partially covered piezoelectric layer. Subsequently, we respectively solved the direct/inverse electro-mechanical problems in Sections 4 and 5. In Section 6, we discussed the size-dependent electro-mechanical response in detail. Finally, in Section 7, we concluded the main conclusions.

2. Theoretical framework

2.1. General formulation

The classical piezoelectric elasticity theory fails to explain the size-dependent electro-mechanical behaviour. The flexoelectric elasticity theory is subsequently developed to describe the size effects phenomenon. The general internal energy density w_0 is written as follows [39,40]

$$w_0 = \frac{1}{2}c_{ijkl}\varepsilon_{ij}\varepsilon_{kl} + \frac{1}{2}g_{ijklpq}\eta_{ijk}\eta_{lpq} + f_{ijkl}P_i\eta_{jkl} + e_{ijkl}Q_{ij}\varepsilon_{kl} + d_{ijk}P_k\varepsilon_{ij} + \frac{1}{2}\alpha_{ij}P_iP_j + \frac{1}{2}b_{ijkl}Q_{ij}Q_{kl} \tag{1}$$

In Eq. (1), c_{ijkl} is the classical fourth-order elastic tensor. g_{ijklpq} is the non-classical sixth-order elastic tensor associated with the strain gradient effects. f_{ijkl} and e_{ijkl} are respectively the direct/converse flexoelectric coefficients. d_{ijk} is the piezoelectric coefficient. α_{ij} and b_{ijkl} are the material constants associated with the polarization effects and polarization gradient effects, respectively. ε_{ij} and η_{ijk} are respectively the strain and strain gradient tensor, and defined as

$$\varepsilon_{ij} = \frac{1}{2}(u_{i,j} + u_{j,i}) \tag{2}$$

$$\eta_{ijk} = \varepsilon_{jk,i} \tag{3}$$

where u_i is the displacement vector and a comma denotes differentiation with respect to the coordinate. P_i and $Q_{ij}(= P_{i,j})$ are the polarization and polarization gradients, respectively.

For the isotropic material, Zhou et al. [20] introduced the orthogonal decomposition of the strain gradient tensor, one is the symmetric/anti-symmetric splitting, other is the hydrostatic/deviatoric splitting, demonstrated the number of independent higher-order material parameters is three, and given the non-classical sixth-order elastic tensor as follows

$$g_{ijklmn} = a_1[(\delta_{ij}\delta_{kl} + \delta_{ik}\delta_{jl})\delta_{mn} + (\delta_{im}\delta_{ln} + \delta_{in}\delta_{lm})\delta_{jk}] + a_2[(\delta_{km}\delta_{ln} + \delta_{kn}\delta_{lm})\delta_{ij} + (\delta_{jm}\delta_{ln} + \delta_{jn}\delta_{lm})\delta_{ik}] + a_3\delta_{il}\delta_{jk}\delta_{mn} + a_4(\delta_{jm}\delta_{kn} + \delta_{jn}\delta_{km})\delta_{il} + a_5[(\delta_{jn}\delta_{kl} + \delta_{jl}\delta_{kn})\delta_{im} + (\delta_{jm}\delta_{kl} + \delta_{jl}\delta_{km})\delta_{in}] \tag{4}$$

where the higher-order material constants $a_n(n = 1, 2, \ldots, 5)$ are derived as

$$a_1 = -\frac{6}{5}\mu l_0^2 - \frac{4}{15}\mu l_1^2 + 2\mu l_2^2 \quad a_2 = \frac{6}{5}\mu l_0^2 - \frac{1}{15}\mu l_1^2 - \mu l_2^2$$
$$a_3 = \frac{9}{5}\mu l_0^2 - \frac{4}{15}\mu l_1^2 - \mu l_2^2 \quad a_4 = \frac{1}{3}\mu l_1^2 + 2\mu l_2^2 \quad a_5 = \frac{2}{3}\mu l_1^2 - 2\mu l_2^2 \tag{5}$$

In Eq. (5), $l_i(i = 0, 1, 2)$ are the independent material length-scale parameters. μ is the shear modulus.

Therefore, according to the Eqs. (1) and (4), the internal energy density w_0 for the flexoelectric elasticity theory with the general strain gradient elasticity is written in the form of strain gradient tensor as follows

$$w_0 = \frac{1}{2}c_{ijkl}\varepsilon_{ij}\varepsilon_{kl} + a_1\eta_{iik}\eta_{kjj} + a_2\eta_{ijj}\eta_{ikk} + a_3\eta_{iik}\eta_{jjk} + a_4\eta_{ijk}\eta_{ijk} + a_5\eta_{ijk}\eta_{kji} + f_{ijkl}P_i\eta_{jkl} + e_{ijkl}Q_{ij}\varepsilon_{kl} + d_{ijk}P_k\varepsilon_{ij} + \frac{1}{2}\alpha_{ij}P_iP_j + \frac{1}{2}b_{ijkl}Q_{ij}Q_{kl} \tag{6}$$

Moreover, based on the hydrostatic and deviatoric splitting of the strain gradient tensor, the internal energy density w_0 can also be expressed in the form of the strain gradient components as follows

$$w_0 = \frac{1}{2}c_{ijkl}\varepsilon_{ij}\varepsilon_{kl} + a_6(\eta^h_{ijk}\eta^h_{ijk} + \eta'^{(2)}_{ijk}\eta'^{(2)}_{ijk}) + a_7\eta^{(1)}_{ijk}\eta^{(1)}_{ijk} + a_8\eta^{as}_{ijk}\eta^{as}_{ijk} + f_{ijkl}P_i(\eta^h_{jkl} + \eta'^{(2)}_{jkl} + \eta^{(1)}_{jkl} + \eta^{as}_{jkl}) + e_{ijkl}Q_{ij}\varepsilon_{kl} + d_{ijk}P_k\varepsilon_{ij} + \frac{1}{2}\alpha_{ij}P_iP_j + \frac{1}{2}b_{ijkl}Q_{ij}Q_{kl} \tag{7}$$

with

$$a_6 = 3\mu l_0^2 \quad a_7 = \mu l_1^2 \quad a_8 = 3\mu l_2^2 \tag{8}$$

where η^h_{ijk}, $\eta'^{(2)}_{ijk}$, $\eta^{(1)}_{ijk}$ and η^{as}_{ijk} are the independent strain gradient components. η^h_{ijk} is the hydrostatic strain gradient component. $\eta'^{(2)}_{ijk}$ is the deviatoric strain gradient component. $\eta^{(1)}_{ijk}$ is the traceless component of the symmetric strain gradient part. η^{as}_{ijk} is symmetric component of the anti-symmetric strain gradient part. The independent strain gradient components are respectively denoted as

$$\eta^h_{ijk} = \frac{1}{3}\delta_{jk}\eta_{inn} \tag{9}$$

$$\eta'^{(2)}_{ijk} = \frac{1}{10}\delta_{ij}(3\eta_{mmk} - \eta_{kmm}) + \frac{1}{10}\delta_{ki}(3\eta_{mmj} - \eta_{jmm}) + \frac{1}{5}\delta_{jk}(2\eta_{imm} - \eta_{mmi}) \tag{10}$$

$$\eta^{(1)}_{ijk} = \frac{1}{3}(\eta_{ijk} + \eta_{jik} + \eta_{kij}) + \frac{1}{15}[\delta_{ij}(2\eta_{mmk} + \eta_{kmm}) + \delta_{ki}(2\eta_{mmj} + \eta_{jmm}) + \delta_{kj}(2\eta_{mmi} + \eta_{imm})] \tag{11}$$

$$\eta^{as}_{ijk} = \frac{1}{3}(e_{ijp}\chi^s_{pk} + e_{ikp}\chi^s_{pj}) \tag{12}$$

In which δ_{ij} is the Kronecker deltas. e_{ijk} is the alternate tensor. χ^s_{ij} is the symmetric rotational gradient component, and defined as

$$\chi^s_{ij} = \frac{1}{2}(\chi_{ij} + \chi_{ji}) \tag{13}$$

where $\chi_{ij} = e_{ipq}\eta_{pqj}$ is the rotational gradients.

2.2. Theory degeneration

The general strain gradient elasticity [20] and the approximated strain gradient elasticity including the modified strain gradient elasticity [18] and the simplified strain gradient elasticity [21,22] were proposed to describe the strain gradient effects. The ability of the flexoelectric elasticity theory incorporating the general or approximated strain gradient elasticity to describe the size-dependent electro-mechanical behaviour is obviously different. Thus, the degeneration analysis of the flexoelectric elasticity theory incorporating the general strain gradient elasticity is performed.

For the flexoelectric elasticity theory incorporating the modified strain gradient elasticity, the modified strain gradient elasticity theory [18] with the dilatation gradients, the deviatoric stretch gradients and the symmetric rotational gradients is used to describe the strain gradient effects. To derive the internal energy density for the flexoelectric elasticity theory with the modified strain gradient elasticity conveniently, the internal energy density for the flexoelectric elasticity theory with the general strain gradient elasticity is expressed in the form of hydrostatic and deviatoric components. According to Eq. (7), neglecting the contributions from the deviatoric strain gradient component $\eta'^{(2)}_{ijk}$, together with the following relations

$$\eta^{h}_{ijk}\eta^{h}_{ijk} = \frac{1}{3}\eta_{inn}\eta_{imm} \tag{14}$$

$$\eta^{as}_{ijk}\eta^{as}_{ijk} = \frac{2}{3}\chi^{s}_{pk}\chi^{s}_{pk} \tag{15}$$

we obtain the internal energy density for the flexoelectric elasticity theory incorporating the modified strain gradient elasticity as

$$\begin{aligned} w_0 &= \frac{1}{2}c_{ijkl}\varepsilon_{ij}\varepsilon_{kl} + a_9\varepsilon_{nn,i}\varepsilon_{mm,i} + a_{10}\eta^{(1)}_{ijk}\eta^{(1)}_{ijk} + a_{11}\chi^{s}_{pk}\chi^{s}_{pk} \\ &+ f_{ijkl}P_i(\eta^{h}_{jkl} + \eta^{(1)}_{jkl} + \eta^{as}_{jkl}) + e_{ijkl}Q_{ij}\varepsilon_{kl} + d_{ijk}P_k\varepsilon_{ij} \\ &+ \frac{1}{2}\alpha_{ij}P_iP_j + \frac{1}{2}b_{ijkl}Q_{ij}Q_{kl} \end{aligned} \tag{16}$$

with

$$a_9 = \mu l_3^2 \quad a_{10} = \mu l_4^2 \quad a_{11} = \mu l_5^2 \tag{17}$$

where $l_3^2 = l_0^2$, $l_4^2 = l_1^2$ and $l_5^2 = 2l_2^2$. The similar internal energy density was also given by Zheng et al. [66]. From the comparison between the Eqs. (7) and (16), it is obviously that the direct flexoelectric effects and the strain gradient effects associated with the deviatoric strain gradient component $\eta'^{(2)}_{ijk}$ are neglected. Moreover, when the flexoelectricity, piezoelectricity, polarization, and polarization gradients are simultaneously ignored, we obtain the strain energy density for the modified strain gradient elasticity theory [18].

For the flexoelectric elasticity theory incorporating the simplified strain gradient elasticity, the simplified strain gradient elasticity theory [21,22] with only part of the strain gradients is applied to describe the strain gradient effects. If the higher-order material constants in Eq. (6) satisfy

$$a_2 = \frac{1}{2}\lambda l_a^2 \quad a_4 = \mu l_a^2 \tag{18}$$

and neglect the contributions from the strain gradients $\eta_{iik}\eta_{kjj}$, $\eta_{iik}\eta_{jjk}$ and $\eta_{ijk}\eta_{kji}$, we obtain the internal energy density for the flexoelectric elasticity theory with the simplified strain gradient elasticity as

$$\begin{aligned} w_0 &= \frac{1}{2}c_{ijkl}\varepsilon_{ij}\varepsilon_{kl} + \frac{1}{2}\lambda l_a^2\eta_{ijj}\eta_{ikk} + \mu l_a^2\eta_{ijk}\eta_{ijk} + f_{ijkl}P_i\eta_{jkl} + e_{ijkl}Q_{ij}\varepsilon_{kl} \\ &+ d_{ijk}P_k\varepsilon_{ij} + \frac{1}{2}\alpha_{ij}P_iP_j + \frac{1}{2}b_{ijkl}Q_{ij}Q_{kl} \end{aligned} \tag{19}$$

In which l_a is the material length-scale parameter. λ and μ are the Lame constants. It can be seen from Eq. (19) that when the material length-scale parameter l_a satisfies $l_a = 0$, we obtain the internal energy density for the flexoelectric elasticity theory without strain gradient effects [58]. Moreover, when the inverse flexoelectricity, piezoelectricity and polarization gradients in Eq. (19) are simultaneously ignored, we obtain the internal energy density for the isotropic flexoelectric elasticity theory [67].

3. Size-dependent electro-mechanical deformation beam

The electro-mechanical deformation beam with a partially covered piezoelectric layer is shown in Fig. 1. The contact between the elastic layer and piezoelectric layer is assumed to be ideal. The non-laminated region displacement field is written as

$$u_x = -z\frac{\partial w(x)}{\partial x} \quad u_y = 0 \quad u_z = w(x) \tag{20}$$

The laminated region displacement field is written as [68]

$$u_x = -(z+d)\frac{\partial w(x)}{\partial x} \quad u_y = 0 \quad u_z = w(x) \tag{21}$$

Where u_x is the x direction displacement component. u_y is the y direction displacement component. u_z is the z direction displacement component. $w(x)$ is the lateral deflection. d is the offset distance of the neutral axis position. The polarization is assumed to occur along the thickness direction, and written as

$$P_x = 0 \quad P_y = 0 \quad P_z = P_z(z) \tag{22}$$

Based on Eqs. (2), (3) and (20), the non-laminated region non-zero strain and strain gradient are respectively derived as

$$\varepsilon_{xx} = -z\frac{\partial^2 w}{\partial x^2} \quad \eta_{xxx} = -z\frac{\partial^3 w}{\partial x^3} \quad \eta_{zxx} = -\frac{\partial^2 w}{\partial x^2} \tag{23}$$

Inserting Eq. (21) into Eqs. (2) and (3), the laminated region non-zero strain and strain gradient are respectively derived as

$$\varepsilon_{xx} = \frac{\partial u_0}{\partial x} - z\frac{\partial^2 w}{\partial x^2} \quad \eta_{xxx} = \frac{\partial^2 u_0}{\partial x^2} - z\frac{\partial^3 w}{\partial x^3} \quad \eta_{zxx} = -\frac{\partial^2 w}{\partial x^2} \tag{24}$$

In Eq. (24), $u_0 = -d \cdot \partial w/\partial x$ is the axial displacement.

For the non-laminated region made of the elastic layer ($0 < x < L_1$), according to Eqs. (1) and (23), the strain energy is derived as

$$U_1 = \frac{1}{2}\int_0^{L_1}\int_{A_{(1)}}[k_1 \cdot (w^{(3)})^2 + s_1 \cdot (w^{(2)})^2]dA_{(1)}dx \tag{25}$$

with

$$s_1 = c_{1111(1)}z^2 + g_{311311(1)} \quad k_1 = g_{111111(1)}z^2 \tag{26}$$

Here, $w^{(2)} = d^2w/dx^2$, $w^{(3)} = d^3w/dx^3$. The material parameters of the lower elastic layer are denoted by the subscript (1). $A_{(1)}$ is the cross section. $c_{1111(1)}$ is the elastic constant. $g_{311311(1)}$ and $g_{111111(1)}$ are the sixth-order elastic tensor and given in Eq. (4). In addition, the non-laminated region ($L_2 < x < L$) strain energy is similar to that in Eq. (25) while the integral scope is from L_2 to L.

For the laminated region made of the piezoelectric layer and elastic layer ($L_1 < x < L_2$), according to Eqs. (1), (22) and (24), the strain energy is derived as

$$\begin{aligned} U_2 = \frac{1}{2}\int_{L_1}^{L_2}&[[A_3 \cdot (w^{(2)})^2 + A_6 \cdot (w^{(3)})^2 + A_1 \cdot (u_0^{(1)})^2 + A_4 \cdot (u_0^{(2)})^2 \\ &- 2A_2 \cdot u_0^{(1)}w^{(2)} - 2e_5 \cdot u_0^{(2)}w^{(3)}] + \int_{A_{(2)}}[\alpha P_3P_3 + b_{3333}\frac{dP_3}{dz}\frac{dP_3}{dz} \\ &- f_{3113}P_3w^{(2)} + f_{1113}P_3(u_0^{(2)} - zw^{(3)}) - f_{3311}\frac{dP_3}{dz}(u_0^{(1)} - zw^{(2)}) \\ &+ d_{113}(u_0^{(1)} - zw^{(2)})P_3]dA_{(2)}]dx \end{aligned} \tag{27}$$

The parameters $A_n (n = 1, 2, \ldots, 6)$ are denoted as

$$\begin{aligned} A_1 &= E_{(1)}A_{(1)} + E_{(2)}A_{(2)} \\ A_2 &= E_{(1)}S_{(1)} + E_{(2)}S_{(2)} \\ A_3 &= E_{(1)}I_{(1)} + \frac{12}{5}\mu_{(1)}l_{0(1)}^2A_{(1)} + \frac{8}{15}\mu_{(1)}l_{1(1)}^2A_{(1)} + 2\mu_{(1)}l_{2(1)}^2A_{(1)} \\ &+ E_{(2)}I_{(2)} + \frac{12}{5}\mu_{(2)}l_{0(2)}^2A_{(2)} + \frac{8}{15}\mu_{(2)}l_{1(2)}^2A_{(2)} + 2\mu_{(2)}l_{2(2)}^2A_{(2)} \\ A_4 &= A_{(1)}(\frac{18}{5}\mu_{(1)}l_{0(1)}^2 + \frac{4}{5}\mu_{(1)}l_{1(1)}^2) + A_{(2)}(\frac{18}{5}\mu_{(2)}l_{0(2)}^2 + \frac{4}{5}\mu_{(2)}l_{1(2)}^2) \\ A_5 &= S_{(1)}(\frac{18}{5}\mu_{(1)}l_{0(1)}^2 + \frac{4}{5}\mu_{(1)}l_{1(1)}^2) + S_{(2)}(\frac{18}{5}\mu_{(2)}l_{0(2)}^2 + \frac{4}{5}\mu_{(2)}l_{1(2)}^2) \\ A_6 &= I_{(1)}(\frac{18}{5}\mu_{(1)}l_{0(1)}^2 + \frac{4}{5}\mu_{(1)}l_{1(1)}^2) + I_{(2)}(\frac{18}{5}\mu_{(2)}l_{0(2)}^2 + \frac{4}{5}\mu_{(2)}l_{1(2)}^2) \end{aligned} \tag{28}$$

Here, $u_0^{(1)} = du_0/dx$, $u_0^{(2)} = d^2u_0/dx^2$. The material parameters of the upper piezoelectric layer are denoted by the subscript (2). $\mu_{(2)}$ is the

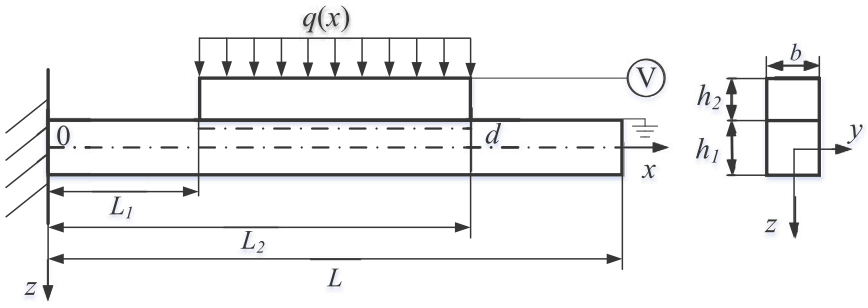

Fig. 1. The laminated microbeam with a partially covered piezoelectric layer.

shear modulus. $E_{(2)}$ is the elasticity modulus. $A_{(2)}$ is the cross section. $l_{i(2)}(i = 0, 1, 2)$ are the material length-scale parameters. $I_{(j)}(j = 1, 2)$ are respectively the moment of inertia of the lower elastic and upper piezoelectric layer. $S_{(j)}(j = 1, 2)$ are the static moment of the lower elastic and upper piezoelectric layer, respectively.

The electric enthalpy of the laminated region ($L_1 < x < L_2$) is written as

$$H_1 = U_2 - \frac{1}{2}\int_{L_1}^{L_2}\int_{A_{(2)}} [\frac{1}{2}\epsilon_0 \frac{d\varphi}{dz}\frac{d\varphi}{dz} + \frac{d\varphi}{dz}P_z]dA_{(2)}dx \tag{29}$$

The work of the laminated region ($L_1 < x < L_2$) is written as

$$W_1 = \frac{1}{2}\int_{L_1}^{L_2} q(x)w(x)dx + [Vw]_{L_1}^{L_2} + [Mw^{(1)}]_{L_1}^{L_2} + [M^h w^{(2)}]_{L_1}^{L_2} \tag{30}$$

where $q(x)$ is the distributed load. V is the shear force. M is the classical moment. M^h is the non-classical moment. In addition, the work of non-laminated region is similar to that in the Eq. (30) while the distributed load $q(x)$ is zero and the integral scope should be from 0 to L_1 or L_2 to L, respectively.

According to the strain energy of the non-laminated region ($0 < x < L_1$) in Eq. (25) and the corresponding work, with the help of the variational principle, the formulation after the variation is derived as

$$\begin{aligned}&\int_0^{L_1}[-k\cdot w^{(6)} + s\cdot w^{(4)}]\delta w dx + [k\cdot w^{(5)} - s\cdot w^{(3)} - V]\delta w|_0^{L_1}\\ &+ [-k\cdot w^{(4)} + s\cdot w^{(2)} - M]\delta w^{(1)}|_0^{L_1} + [-M^h + k\cdot w^{(3)}]\delta w^{(2)}|_0^{L_1} = 0\end{aligned} \tag{31}$$

with

$$s = c_{1111(1)}I_{(1)} + g_{311311(1)} \quad k = g_{111111(1)}I_{(1)} \tag{32}$$

From Eq. (31), the bending governing equation is obtained as

$$-k\cdot w^{(6)} + s\cdot w^{(4)} = 0 \tag{33}$$

The bending boundary conditions are obtained as

$$\begin{aligned}&-s\cdot w^{(3)} + k\cdot w^{(5)} = V\\ &or \quad w = \bar{w} \quad when \quad x = 0 \quad and \quad x = L_1\end{aligned} \tag{34}$$

$$\begin{aligned}&-k\cdot w^{(4)} + s\cdot w^{(2)} = M\\ &or \quad w^{(1)} = \bar{w}^{(1)} \quad when \quad x = 0 \quad and \quad x = L_1\end{aligned} \tag{35}$$

$$\begin{aligned}&k\cdot w^{(3)} = M^h\\ &or \quad w^{(2)} = \bar{w}^{(2)} \quad when \quad x = 0 \quad and \quad x = L_1\end{aligned} \tag{36}$$

The non-laminated region ($L_2 < x < L$) governing equation is same as that in Eq. (33). The corresponding boundary conditions can also be obtained from Eqs. (34)–(36) when $x = L_2$ and $x = L$. It can be seen from Eqs. (7), (16) and (17) that by taking $l_3^2 = l_0^2$, $l_4^2 = l_1^2$ and $l_5^2 = 2l_2^2$, the governing equation and boundary conditions of the general strain gradient elasticity in Eq. (31)–(36) can reduce to that of the modified strain gradient elasticity. From Eqs. (7), (18) and (19), it can be seen that by taking $l_0^2 = l_2^2$, $l_1^2 = 3l_2^2$ and $l_a^2 = 3l_2^2$, the governing equation and boundary conditions of the general strain gradient elasticity in Eq. (31)–(36) can also reduce to that of the modified strain gradient elasticity [25].

Similarly, based on the electric enthalpy of the laminated region ($L_1 < x < L_2$) in Eq. (29), the work in Eq. (30) and the variational principle, the formulation after the variation is obtained. For brevity, the formulation was shown in Eq. (A.1) in Appendix A. From Eq. (A.1), the electro-mechanical coupling governing equations of the laminated region ($L_1 < x < L_2$) are derived as

$$\begin{aligned}&A_3\cdot w^{(4)} - A_6\cdot w^{(6)} + A_5\cdot u_0^{(5)} - A_2\cdot u_0^{(3)} + \int_{A_{(2)}}[-f_{3113}\frac{d^2P_3}{dx^2}\\ &+ f_{3311}z\frac{d^3P_3}{dx^2dz} + f_{1113}\frac{d^3P_3}{dx^3}z - d_{113}z\frac{d^2P_3}{dx^2}]dA_{(2)} - q(x) = 0\end{aligned} \tag{37}$$

$$\begin{aligned}&A_2\cdot w^{(3)} - A_5\cdot w^{(5)} + A_4\cdot u_0^{(4)} - A_1\cdot u_0^{(2)} + \int_{A_{(2)}}[f_{1113}\frac{d^2P_3}{dx^2}\\ &+ f_{3311}\frac{d^2P_3}{dxdz} - d_{113}\frac{dP_3}{dx}]dA_{(2)} = 0\end{aligned} \tag{38}$$

The electric governing equations of the laminated region ($L_1 < x < L_2$) are derived as

$$\begin{aligned}&\alpha P_3 - b_{33}\frac{d^2P_3}{dz^2} + f_{1113}(u_0^{(2)} - zw^{(3)}) - f_{3113}w^{(2)} - f_{3311}w^{(2)} + \frac{d\varphi}{dz}\\ &+ d_{113}(u_0^{(1)} - zw^{(2)}) = 0\end{aligned} \tag{39}$$

$$-\epsilon_0\frac{d^2\varphi}{dz^2} + \frac{dP_3}{dz} = 0 \tag{40}$$

From Eqs. (37)–(40), it should be noted that the terms with the coefficients f_{3113} or f_{1113} represent the influences from the direct flexoelectric effects respectively induced from the strain gradients η_{zxx} and η_{xxx}. The terms with the coefficient f_{3311} represent the influences from the inverse flexoelectric effects induced from the polarization gradient $P_{z,z}$. The terms with the coefficient d_{113} represent the influences from the piezoelectric effects. The shear force boundary condition is derived as

$$\begin{aligned}&-A_3\cdot w^{(3)} + A_6\cdot w^{(5)} - A_5\cdot u_0^{(4)} + A_2\cdot u_0^{(2)} + \int_{A_{(2)}}[f_{3113}\frac{dP_3}{dx}\\ &- f_{3311}z\frac{d^2P_3}{dxdz} - f_{1113}\frac{d^2P_3}{dx^2}z + d_{113}z\frac{dP_3}{dx}]dA_{(2)} = V\\ &or \quad w = \bar{w} \quad when \quad x = L_1 \quad and \quad x = L_2\end{aligned} \tag{41}$$

The moment boundary condition is derived as

$$\begin{aligned}&A_3\cdot w^{(2)} - A_6\cdot w^{(4)} + A_5\cdot u_0^{(3)} - A_2\cdot u_0^{(1)} + \int_{A_{(2)}}[-f_{3113}P_3 + f_{3311}z\frac{dP_3}{dz}\\ &+ f_{1113}\frac{dP_3}{dx}z - d_{113}zP_3]dA_{(2)} = M\\ &or \quad w^{(1)} = \bar{w}^{(1)} \quad when \quad x = L_1 \quad and \quad x = L_2\end{aligned} \tag{42}$$

The non-classical moment boundary condition is derived as

$$\begin{aligned}&A_6\cdot w^{(3)} - A_5\cdot u_0^{(2)} - f_{1113}zP_3 = M^h\\ &or \quad w^{(2)} = \bar{w}^{(2)} \quad when \quad x = L_1 \quad and \quad x = L_2\end{aligned} \tag{43}$$

The axial force boundary condition is derived as

$$-A_2\cdot w^{(2)}+A_5\cdot w^{(4)}-A_4\cdot u_0^{(3)}+A_1\cdot u_0^{(1)}+\int_{A_{(2)}}[-f_{1113}\frac{dP_3}{dx}-f_{3311}\frac{dP_3}{dz}+d_{113}P_3]dA_{(2)}=0 \quad or \quad u_0=\bar{u}_0 \quad when \quad x=L_1 \quad and \quad x=L_2 \tag{44}$$

The non-classical axial force boundary condition is derived as

$$-A_5\cdot w^{(3)}+A_4\cdot u_0^{(2)}+f_{1113}P_3=0 \quad or \quad u_0^{(1)}=\bar{u}_0^{(1)} \quad when \quad x=L_1 \quad and \quad x=L_2 \tag{45}$$

The electric boundary conditions are derived as

$$b_{33}\frac{dP_3}{dz}+f_{3311}zw^{(2)}-f_{3311}u_0^{(1)}=0 \quad or \quad P_3=\bar{P}_3 \quad when \quad z=-(h_2+\frac{h_1}{2}) \quad and \quad z=-\frac{h_1}{2} \tag{46}$$

$$-\varepsilon_0\frac{d\varphi}{dz}+P_3=0 \quad or \quad \varphi=\bar{\varphi}_3 \quad when \quad z=-(h_2+\frac{h_1}{2}) \quad and \quad z=-\frac{h_1}{2} \tag{47}$$

It should be noted that the governing equations and boundary conditions of the extended flexoelectric theory with general strain gradient elasticity in Eq. (37)–(47) can respectively reduce to that of the extended flexoelectric theory with modified or simplified strain gradient elasticity when the material length-scale parameters satisfy $l_3^2=l_0^2$, $l_4^2=l_1^2$ and $l_5^2=2l_2^2$, or $l_0^2=l_2^2$, $l_1^2=3l_2^2$ and $l_a^2=3l_2^2$ [25].

It can be seen from Eqs. (33)–(47) that the present model with the strain gradients and flexoelectricity can describe the size-dependent electro-mechanical response. When the piezoelectricity is ignored, the present model will reduce to the beam model with strain gradients and flexoelectricity [45]. When the piezoelectricity and flexoelectricity are further ignored, the present model will reduce to the beam model with only strain gradients [68]. Moreover, when the piezoelectricity, flexoelectricity and strain gradients are ignored simultaneously, the classical beam model is obtained.

4. Direct electro-mechanical problem

For a microbeam subjected with the uniformly distributed load q along the laminated region ($L_1<x<L_2$), the electric governing equations are obtained from Eqs. (39) and (40) as

$$\alpha P_3-b_{33}\frac{d^2P_3}{dz^2}+f_{1113}(u_0^{(2)}-zw^{(3)})-f_{3113}w^{(2)}-f_{3311}w^{(2)}+\frac{d\varphi}{dz}+d_{113}(u_0^{(1)}-zw^{(2)})=0 \tag{48}$$

$$-\varepsilon_0\frac{d^2\varphi}{dz^2}+\frac{dP_3}{dz}=0 \tag{49}$$

The electric boundary conditions are obtained from Eqs. (46) and (47) as

$$\varphi|_{z=-\frac{h_1}{2}}=0 \quad [-\varepsilon_0\frac{d\varphi}{dz}+P_3]|_{z=-(h_2+\frac{h_1}{2})}=0 \tag{50}$$

$$[b_{33}\frac{dP_3}{dz}+f_{3311}zw^{(2)}-f_{3311}u_0^{(1)}]|_{z=-\frac{h_1}{2}}=0 \quad [b_{33}\frac{dP_3}{dz}+f_{3311}zw^{(2)}-f_{3311}u_0^{(1)}]|_{z=-(h_2+\frac{h_1}{2})}=0 \tag{51}$$

According to Eqs. (48) and (49), the induced polarization P_3 and induced electric potential φ are respectively derived as

$$P_3=c_1+c_2e^{gz}+c_3e^{-gz}+\frac{f_{1113}\varepsilon_0w^{(3)}}{(1+\alpha\varepsilon_0)}z+\frac{d_{113}\varepsilon_0w^{(2)}}{(1+\alpha\varepsilon_0)}z \tag{52}$$

$$\varphi=c_4+c_5z+\frac{c_2}{g\varepsilon_0}e^{gz}-\frac{c_3}{g\varepsilon_0}e^{-gz}+\frac{f_{1113}w^{(3)}}{2(1+\alpha\varepsilon_0)}z^2+\frac{d_{113}w^{(2)}}{2(1+\alpha\varepsilon_0)}z^2 \tag{53}$$

In Eqs. (52) and (53), $c_n(n=1,2,3,4,5)$ are unknown constants to be determined. Substituting the induced polarization of Eq. (52) and induced electric potential of Eq. (53) into the electric boundary conditions in Eqs. (50)–(51), the unknown constants are determined and shown in Appendix B. The induced polarization P_3 and induced electric potential φ are respectively derived as

$$\begin{aligned}P_3=&\frac{2f_{3113}\varepsilon_0w^{(2)}}{(1+\alpha\varepsilon_0)}-\frac{f_{1113}\varepsilon_0u_0^{(2)}}{(1+\alpha\varepsilon_0)}-\frac{d_{113}\varepsilon_0u_0^{(1)}}{(1+\alpha\varepsilon_0)}+\frac{f_{1113}\varepsilon_0w^{(3)}}{(1+\alpha\varepsilon_0)}z\\&+\frac{\varepsilon_0f_{1113}w^{(3)}}{g(1+\alpha\varepsilon_0)}(A_{s1}e^{gz}+A_{s4}e^{-gz})+\frac{f_{3311}\varepsilon_0gh_1w^{(2)}}{2(1+\alpha\varepsilon_0)}(A_{s2}e^{gz}+A_{s5}e^{-gz})\\&+\frac{f_{3311}\varepsilon_0g(h_2+\frac{h_1}{2})w^{(2)}}{(1+\alpha\varepsilon_0)}(-A_{s3}e^{gz}-A_{s6}e^{-gz})+\frac{d_{113}\varepsilon_0w^{(2)}}{(1+\alpha\varepsilon_0)}z\\&+\frac{f_{3311}g\varepsilon_0u_0^{(1)}}{(1+\alpha\varepsilon_0)}(-A_{s1}e^{gz}-A_{s4}e^{-gz})+\frac{d_{31}\varepsilon_0w^{(2)}}{g(1+\alpha\varepsilon_0)}(A_{s1}e^{gz}+A_{s4}e^{-gz})\end{aligned} \tag{54}$$

$$\begin{aligned}\varphi=&[\frac{b_{33}f_{1113}\varepsilon_0}{(1+\alpha\varepsilon_0)^2}-\frac{f_{1113}h_1^2}{8(1+\alpha\varepsilon_0)}]w^{(3)}+[\frac{f_{3311}h_1}{2(1+\alpha\varepsilon_0)}+\frac{b_{33}d_{31}\varepsilon_0}{(1+\alpha\varepsilon_0)^2}\\&-\frac{d_{31}h_1^2}{8(1+\alpha\varepsilon_0)}]w^{(2)}-\frac{f_{1113}h_1}{2(1+\alpha\varepsilon_0)}u_0^{(2)}-[\frac{d_{31}h_1}{2(1+\alpha\varepsilon_0)}+\frac{f_{3311}}{(1+\alpha\varepsilon_0)}]u_0^{(1)}\\&+\frac{2f_{3113}}{(1+\alpha\varepsilon_0)}zw^{(2)}-\frac{f_{1113}}{(1+\alpha\varepsilon_0)}zu_0^{(2)}-\frac{d_{113}}{(1+\alpha\varepsilon_0)}zu_0^{(1)}+\frac{d_{113}}{2(1+\alpha\varepsilon_0)}z^2w^{(2)}\\&+\frac{f_{1113}w^{(3)}}{g^2(1+\alpha\varepsilon_0)}(A_{s1}e^{gz}-A_{s4}e^{-gz})+\frac{f_{3311}h_1w^{(2)}}{2(1+\alpha\varepsilon_0)}(A_{s2}e^{gz}-A_{s5}e^{-gz})\\&+\frac{f_{3311}(h_2+\frac{h_1}{2})w^{(2)}}{(1+\alpha\varepsilon_0)}(-A_{s3}e^{gz}+A_{s6}e^{-gz})+\frac{f_{1113}}{2(1+\alpha\varepsilon_0)}z^2w^{(3)}\\&+\frac{f_{3311}u_0^{(1)}}{(1+\alpha\varepsilon_0)}(-A_{s1}e^{gz}+A_{s4}e^{-gz})+\frac{d_{31}w^{(2)}}{g^2(1+\alpha\varepsilon_0)}(A_{s1}e^{gz}-A_{s4}e^{-gz})\end{aligned} \tag{55}$$

In Eqs. (54) and (55), the parameters $A_{sn}(n=1,2,\ldots,6)$ are defined as follows

$$\begin{aligned}A_{s1}&=\frac{(1-e^{gh_2})}{(e^{g(h_2-\frac{h_1}{2})}-e^{-g(h_2+\frac{h_1}{2})})} \quad A_{s2}=\frac{e^{gh_2}}{(e^{g(h_2-\frac{h_1}{2})}-e^{-g(h_2+\frac{h_1}{2})})}\\A_{s3}&=\frac{1}{(e^{g(h_2-\frac{h_1}{2})}-e^{-g(h_2+\frac{h_1}{2})})} \quad A_{s4}=\frac{(1-e^{-gh_2})}{(e^{g(h_2+\frac{h_1}{2})}-e^{g(\frac{h_1}{2}-h_2)})}\\A_{s5}&=\frac{e^{-gh_2}}{(e^{g(h_2+\frac{h_1}{2})}-e^{g(\frac{h_1}{2}-h_2)})} \quad A_{s6}=\frac{1}{(e^{g(h_2+\frac{h_1}{2})}-e^{g(\frac{h_1}{2}-h_2)})}\end{aligned} \tag{56}$$

with

$$g=\sqrt{\frac{(1+\alpha\varepsilon_0)}{b_{33}\varepsilon_0}} \tag{57}$$

For the mechanical governing equations of the laminated region ($L_1<x<L_2$), substituting the induced polarization of Eq. (54) into the electro-mechanical coupling governing equations of Eqs. (37) and (38), the following equations are derived as

$$a_3\cdot w^{(4)}+a_6\cdot w^{(6)}+a_5\cdot u_0^{(5)}+T_4\cdot u_0^{(4)}+a_7\cdot u_0^{(3)}=q \tag{58}$$

$$a_2\cdot w^{(3)}+T_{10}\cdot w^{(4)}+a_8\cdot w^{(5)}+a_4\cdot u_0^{(4)}+a_1\cdot u_0^{(2)}=0 \tag{59}$$

Similarly, according to the induced polarization in Eq. (54) and the boundary conditions in Eqs. (41)–(45), the mechanical boundary conditions of the laminated region ($L_1<x<L_2$) are derived as

$$-a_3\cdot w^{(3)}-a_6\cdot w^{(5)}-a_5\cdot u_0^{(4)}-T_4\cdot u_0^{(3)}-a_7\cdot u_0^{(2)}=V \quad or \quad w=\bar{w} \quad when \quad x=L_1 \quad and \quad x=L_2 \tag{60}$$

$$a_3\cdot w^{(2)}+a_6\cdot w^{(4)}+a_5\cdot u_0^{(3)}+T_4\cdot u_0^{(2)}+a_7\cdot u_0^{(1)}=M \quad or \quad w^{(1)}=\bar{w}^{(1)} \quad when \quad x=L_1 \quad and \quad x=L_2 \tag{61}$$

$$-a_6\cdot w^{(3)}-a_5\cdot u_0^{(2)}-T_6\cdot w^{(2)}-T_7\cdot u_0^{(1)}=M^h \quad or \quad w^{(2)}=\bar{w}^{(2)} \quad when \quad x=L_1 \quad and \quad x=L_2 \tag{62}$$

$$-a_2\cdot w^{(2)}-a_8\cdot w^{(4)}-a_4\cdot u_0^{(3)}-T_{10}\cdot w^{(3)}-a_1\cdot u_0^{(1)}=0 \quad or \quad u_0=\bar{u}_0 \quad when \quad x=L_1 \quad and \quad x=L_2 \tag{63}$$

$$a_8\cdot w^{(3)}+a_4\cdot u_0^{(2)}+T_{13}\cdot w^{(2)}+T_{14}\cdot u_0^{(1)}=0 \quad or \quad u_0^{(1)}=\bar{u}_0^{(1)} \quad when \quad x=L_1 \quad and \quad x=L_2 \tag{64}$$

Here, the parameters $a_n(n=1,2,\ldots,7)$ in Eqs. (58)–(64) are defined as follows

$$a_1=-A_1+T_{12}\quad a_2=A_2+T_8\quad a_3=A_3+T_1\quad a_4=A_4+T_{11}$$
$$a_5=A_5+T_3\quad a_6=-A_6+T_2\quad a_7=-A_2+T_5\quad a_8=-A_5+T_9 \tag{65}$$

For brevity, the parameters $T_n(n=1,2,\ldots,14)$ in the direct electromechanical governing equations of Eqs. (58)–(59) and boundary conditions of Eqs. (60)–(65) are given in Appendix C.

According to the mechanical governing equations in Eqs. (58) and (59), together with the operator method, the deflection and axial displacement solution for the laminated region ($L_1<x<L_2$) are derived as

$$w_1(x)=c_6+c_7x+c_8x^2+c_9x^3+\frac{qa_1}{24(a_1a_3-a_2a_7)}x^4+c_{10}e^{r_1x}+c_{11}e^{r_2x}+c_{12}e^{r_3x}+c_{13}e^{r_4x} \tag{66}$$

$$u_0(x)=c_{14}+c_{15}x+(-\frac{3a_2}{a_1}c_9-\frac{qT_{10}}{2(a_1a_3-a_2a_7)})x^2+\frac{qa_2}{6}x^3+\frac{(-a_3r_1^4-a_6r_1^6)}{(-a_8r_1^5+T_4r_1^4+a_7r_1^3)}c_{10}e^{r_1x}+\frac{(-a_3r_2^4-a_6r_2^6)}{(-a_8r_2^5+T_4r_2^4+a_7r_2^3)}c_{11}e^{r_2x}+\frac{(-a_3r_3^4-a_6r_3^6)}{(-a_8r_3^5+T_4r_3^4+a_7r_3^3)}c_{12}e^{r_3x}+\frac{(-a_3r_4^4-a_6r_4^6)}{(-a_8r_4^5+T_4r_4^4+a_7r_4^3)}c_{13}e^{r_4x} \tag{67}$$

with

$$r_1=-\frac{m_2}{4m_1}+\sqrt{m_6}+\sqrt{-m_6-\frac{P}{2}+2\sqrt{m_6^2+\frac{1}{2}Pm_6+\frac{1}{16}(P^2-4R)}}$$
$$r_2=-\frac{m_2}{4m_1}+\sqrt{m_6}-\sqrt{-m_6-\frac{P}{2}+2\sqrt{m_6^2+\frac{1}{2}Pm_6+\frac{1}{16}(P^2-4R)}}$$
$$r_3=-\frac{m_2}{4m_1}-\sqrt{m_6}+\sqrt{-m_6-\frac{P}{2}-2\sqrt{m_6^2+\frac{1}{2}Pm_6+\frac{1}{16}(P^2-4R)}} \tag{68}$$
$$r_4=-\frac{m_2}{4m_1}-\sqrt{m_6}-\sqrt{-m_6-\frac{P}{2}-2\sqrt{m_6^2+\frac{1}{2}Pm_6+\frac{1}{16}(P^2-4R)}}$$

The derive process is given in Appendix C. In Eq. (68), the parameters are defined as

$$m_1=a_6a_4+a_5^2$$
$$m_2=-T_{10}a_5+T_4a_5$$
$$m_3=a_3a_4+a_6a_1+a_2a_8-T_{10}T_4-a_7a_8$$
$$m_4=-a_2T_4-T_{10}a_7$$
$$m_5=a_3a_7-a_2a_7$$
$$m_6=-\frac{P}{6}+\sqrt[3]{m_7+\sqrt{m_8}}+\sqrt[3]{m_7-\sqrt{m_8}}$$
$$m_7=\frac{(-72PR+27Q^2+2P^3)}{3456}$$
$$m_8=(\frac{72PR-27Q^2-2P^3}{3456})^2-(\frac{P^2+12R}{144})^3 \tag{69}$$
$$P=\frac{(8m_1m_3-3m_2^2)}{8m_1^2}$$
$$Q=\frac{(m_2^3-4m_1m_2m_3+8m_1^2m_4)}{8m_1^3}$$
$$R=\frac{(16m_1m_2^3m_3-3m_2^4-64m_1^2m_2m_4+256m_1^3m_5)}{256m_1^4}$$

According to the mechanical governing equations of the non-laminated region ($0<x<L_1$) in the Eq. (33), using the reduction method, the non-laminated region ($0<x<L_1$) deflection is easily derived as

$$w_2(x)=c_{16}+c_{17}x+c_{18}x^2+c_{19}x^3+c_{20}e^{\sqrt{\frac{s}{k}}x}+c_{21}e^{-\sqrt{\frac{s}{k}}x} \tag{70}$$

Similarly, the non-laminated region ($L_2<x<L$) deflection is derived as

$$w_3(x)=c_{22}+c_{23}x+c_{24}x^2+c_{25}x^3+c_{26}e^{\sqrt{\frac{s}{k}}x}+c_{27}e^{-\sqrt{\frac{s}{k}}x} \tag{71}$$

The deflection in Eqs. (66), (70) and (71), and axial displacement in Eq. (67) with unknown constants $c_n(n=6,7,\ldots,27)$ can be determined by using the equilibrium conditions of internal forces, the deformation compatibility conditions and the boundary conditions. For the equilibrium conditions of shear force at the conjunction, the following equations are given

$$\begin{aligned}&-s\cdot w_2^{(3)}(L_1)+k\cdot w_2^{(5)}(L_1)=-a_3\cdot w_1^{(3)}(L_1)-a_6\cdot w_1^{(5)}(L_1)\\&-a_5\cdot u_0^{(4)}(L_1)-T_4\cdot u_0^{(3)}(L_1)-a_7\cdot u_0^{(2)}(L_1)\\&-a_3\cdot w_1^{(3)}(L_2)-a_6\cdot w_1^{(5)}(L_2)-a_5\cdot u_0^{(4)}(L_2)-T_4\cdot u_0^{(3)}(L_2)\\&-a_7\cdot u_0^{(2)}(L_2)=-s\cdot w_3^{(3)}(L_2)+k\cdot w_3^{(5)}(L_2)\end{aligned} \tag{72}$$

For the equilibrium conditions of moment at the conjunction, the following equations are given

$$\begin{aligned}&s\cdot w_2^{(2)}(L_1)-k\cdot w_2^{(4)}(L_1)=a_3\cdot w_1^{(2)}(L_1)+a_6\cdot w_1^{(4)}(L_1)\\&+a_5\cdot u_0^{(3)}(L_1)+T_4\cdot u_0^{(2)}(L_1)+a_7\cdot u_0^{(1)}(L_1)\\&a_3\cdot w_1^{(2)}(L_2)+a_6\cdot w_1^{(4)}(L_2)+a_5\cdot u_0^{(3)}(L_2)+T_4\cdot u_0^{(2)}(L_2)\\&+a_7\cdot u_0^{(1)}(L_2)=s\cdot w_3^{(2)}(L_2)-k\cdot w_3^{(4)}(L_2)\end{aligned} \tag{73}$$

For the equilibrium conditions of non-classical moment at the conjunction, the following equations are given

$$\begin{aligned}&k\cdot w_2^{(3)}(L_1)=-a_6\cdot w_1^{(3)}(L_1)-a_5\cdot u_0^{(2)}(L_1)\\&-T_6\cdot w_1^{(2)}(L_1)-T_7\cdot u_0^{(1)}(L_1)\\&-a_6\cdot w_1^{(3)}(L_2)-a_5\cdot u_0^{(2)}(L_2)-T_6\cdot w_1^{(2)}(L_2)\\&-T_7\cdot u_0^{(1)}(L_2)=k\cdot w_3^{(3)}(L_2)\end{aligned} \tag{74}$$

For the deformation compatibility conditions at the conjunction, the following equations are given

$$\begin{aligned}&w_2(L_1)=w_1(L_1)\quad u_0(L_1)=0\quad w_2^{(1)}(L_1)=w_1^{(1)}(L_1)\\&w_2^{(2)}(L_1)=w_1^{(2)}(L_1)\quad u_0^{(1)}(L_1)=0\\&w_1(L_2)=w_3(L_2)\quad u_0(L_2)=0\quad w_1^{(1)}(L_2)=w_3^{(1)}(L_2)\\&w_1^{(2)}(L_2)=w_3^{(2)}(L_2)\quad u_0^{(1)}(L_2)=0\end{aligned} \tag{75}$$

For a beam with one end is free and the other end is clamped, the boundary conditions are written as follows

$$\begin{aligned}&w_2^{(1)}(0)=0\quad w_2(0)=0\quad w_2^{(2)}(L)=0\quad w_3^{(2)}(0)=0\\&s\cdot w_3^{(2)}(L)-k\cdot w_3^{(4)}(L)=0\quad -s\cdot w_3^{(3)}(L)+k\cdot w_3^{(5)}(L)=0\end{aligned} \tag{76}$$

According to the deflection in Eqs. (66), (70) and (71), and axial displacement in Eq. (67), together with the equilibrium conditions of internal forces in Eqs. (72)–(74), the deformation compatibility conditions in Eq. (75) and the cantilever boundary conditions in Eq. (76), the deflection and axial displacement solution for the cantilever piezoelectric microbeam is obtained. Then, based on the obtained deflection and axial displacement, together with Eqs. (54) and (55), the induced polarization and induced electric potential are determined. Moreover, the density of the charge induced from the piezoelectric layer can be written as

$$\rho(x)=C\varphi(x) \tag{77}$$

Here, C is the capacitance per unit surface, $C=\varepsilon_r\varepsilon_0/h_2$. ε_r is the relative dielectric constant. ε_0 is the vacuum constant. The collected

charge of the piezoelectric layer is derived as

$$Q(x) = b_2 \int_{L_1}^{L_2} |\rho - (h_2 + \frac{1}{2}h_1)| dx$$
$$= b_2 C|[\frac{b_{33} f_{1113} \varepsilon_0}{(1+\alpha\varepsilon_0)^2} - \frac{f_{1113}}{g^2(1+\alpha\varepsilon_0)} + \frac{f_{1113} h_2 (h_2+h_1)}{2(1+\alpha\varepsilon_0)}]$$
$$[w_1^{(2)}(L_2) - w_1^{(2)}(L_1)]| + b_2 C|[-\frac{f_{3311} h_2}{(1+\alpha\varepsilon_0)} + \frac{b_{33} d_{31} \varepsilon_0}{(1+\alpha\varepsilon_0)^2} - \frac{d_{31}}{g^2(1+\alpha\varepsilon_0)}$$
$$+ \frac{d_{31} h_2 (h_2+h_1)}{2(1+\alpha\varepsilon_0)}][w_1^{(1)}(L_2) - w_1^{(1)}(L_1)]| + b_2 C|\frac{f_{1113} h_2}{(1+\alpha\varepsilon_0)}[u_0^{(1)}(L_2)$$
$$- u_0^{(1)}(L_1)]| + b_2 C|\frac{b d_{31} h_2}{(1+\alpha\varepsilon_0)}[u_0(L_2) - u_0(L_1)]| \tag{78}$$

Thus, the polarization, electric potential and collected charge induced from the direct electro-mechanical process are obtained. The direct electro-mechanical response of the cantilever piezoelectric microbeam is determined. Similarly, the direct electro-mechanical problem of the piezoelectric microbeam under other boundary conditions can also be solved.

5. Inverse electro-mechanical problem

For a microbeam subjected with the external voltage V along the thickness direction of the piezoelectric layer, the electric governing equations are obtained from Eqs. (39) and (40) as

$$\alpha P_3 - b_{33}\frac{d^2 P_3}{dz^2} + f_{1113}(u_0^{(2)} - z w^{(3)}) - f_{3113} w^{(2)} - f_{3311} w^{(2)} + \frac{d\varphi}{dz}$$
$$+ d_{113}(u_0^{(1)} - z w^{(2)}) = 0 \tag{79}$$
$$-\varepsilon_0 \frac{d^2\varphi}{dz^2} + \frac{dP_3}{dz} = 0 \tag{80}$$

The electric boundary conditions are obtained from Eqs. (46) and (47) as

$$\varphi|_{z=-\frac{h_1}{2}} = 0 \quad \varphi|_{z=-(h_2+\frac{h_1}{2})} = V \tag{81}$$

$$[b_{33}\frac{dP_3}{dz} + f_{3311} z w^{(2)} - f_{3311} u_0^{(1)}]|_{z=-\frac{h_1}{2}} = 0$$
$$[b_{33}\frac{dP_3}{dz} + f_{3311} z w^{(2)} - f_{3311} u_0^{(1)}]|_{z=-(h_2+\frac{h_1}{2})} = 0 \tag{82}$$

According to the Eqs. (79) and (80), the induced polarization P_3 and induced electric potential φ are respectively derived as

$$P_3 = b_1 + b_2 e^{gz} + b_3 e^{-gz} + \frac{f_{1113}\varepsilon_0 w^{(3)}}{(1+\alpha\varepsilon_0)} z + \frac{d_{113}\varepsilon_0 w^{(2)}}{(1+\alpha\varepsilon_0)} z \tag{83}$$

$$\varphi = b_4 + b_5 z + \frac{b_2}{g\varepsilon_0} e^{gz} - \frac{b_3}{g\varepsilon_0} e^{-gz} + \frac{f_{1113} w^{(3)}}{2(1+\alpha\varepsilon_0)} z^2 + \frac{d_{113} w^{(2)}}{2(1+\alpha\varepsilon_0)} z^2 \tag{84}$$

Here, $b_n (n = 1, 2, 3, 4, 5)$ are constants to be determined. Inserting the induced polarization of Eqs. (83) and induced electric potential of (84) into the electric boundary conditions in Eqs. (81)–(82), the constants are determined and shown in Appendix D. Therefore, the induced polarization P_3 and induced electric potential φ are respectively written as

$$P_3 = (\frac{2 f_{3113}}{\alpha} - \frac{f_{3113}}{\alpha(1+\alpha\varepsilon_0)} - \frac{d_{31}(h_2+h_1)}{2\alpha(1+\alpha\varepsilon_0)}) w^{(2)} - \frac{f_{1113}(h_2+h_1)}{2\alpha(1+\alpha\varepsilon_0)} w^{(3)}$$
$$- \frac{f_{1113}}{\alpha} u_0^{(2)} - \frac{d_{31}}{\alpha} u_0^{(1)} + \frac{V}{h_2 \alpha} + \frac{f_{1113}\varepsilon_0 w^{(3)}}{(1+\alpha\varepsilon_0)} z + \frac{d_{113}\varepsilon_0 w^{(2)}}{(1+\alpha\varepsilon_0)} z$$
$$+ \frac{\varepsilon_0 f_{1113} w^{(3)}}{g(1+\alpha\varepsilon_0)}(A_{s1} e^{gz} + A_{s4} e^{-gz}) + \frac{f_{3311}\varepsilon_0 g h_1 w^{(2)}}{2(1+\alpha\varepsilon_0)}(A_{s2} e^{gz} + A_{s5} e^{-gz})$$
$$+ \frac{f_{3311}\varepsilon_0 g(h_2 + \frac{h_1}{2}) w^{(2)}}{(1+\alpha\varepsilon_0)}(-A_{s3} e^{gz} - A_{s6} e^{-gz}) + \frac{f_{3311} g \varepsilon_0 u_0^{(1)}}{(1+\alpha\varepsilon_0)}$$
$$(-A_{s1} e^{gz} - A_{s4} e^{-gz}) + \frac{d_{31}\varepsilon_0 w^{(2)}}{g(1+\alpha\varepsilon_0)}(A_{s1} e^{gz} + A_{s4} e^{-gz}) \tag{85}$$

$$\varphi = [\frac{f_{1113} h_1 (2h_2+h_1)}{8(1+\alpha\varepsilon_0)} + \frac{f_{1113} b_{33}\varepsilon_0}{(1+\alpha\varepsilon_0)^2}] w^{(3)} - \frac{V h_1}{2h_2} + [\frac{b_{33} d_{31}\varepsilon_0}{(1+\alpha\varepsilon_0)^2}$$
$$+ \frac{d_{31} h_1 (2h_2+h_1)}{8(1+\alpha\varepsilon_0)}] w^{(2)} - \frac{f_{3311}}{(1+\alpha\varepsilon_0)} u_0^{(1)} + [\frac{f_{3311}}{(1+\alpha\varepsilon_0)}$$
$$+ \frac{d_{31}(h_2+h_1)}{2(1+\alpha\varepsilon_0)}] w^{(2)} z + \frac{f_{1113}(h_2+h_1)}{2(1+\alpha\varepsilon_0)} z w^{(3)} - \frac{V}{h_2} z$$
$$+ \frac{f_{1113}}{2(1+\alpha\varepsilon_0)} z^2 w^{(2)} + \frac{d_{31}}{2(1+\alpha\varepsilon_0)} z^2 w^{(2)} + \frac{f_{1113} w^{(3)}}{g^2(1+\alpha\varepsilon_0)}$$
$$(A_{s1} e^{gz} - A_{s4} e^{-gz}) + \frac{f_{3311} h_1 w^{(2)}}{2(1+\alpha\varepsilon_0)}(A_{s2} e^{gz} - A_{s5} e^{-gz})$$
$$+ \frac{f_{3311}(h_2 + \frac{h_1}{2}) w^{(2)}}{(1+\alpha\varepsilon_0)}(-A_{s3} e^{gz} + A_{s6} e^{-gz}) + \frac{f_{3311} u_0^{(1)}}{(1+\alpha\varepsilon_0)}$$
$$(-A_{s1} e^{gz} + A_{s4} e^{-gz}) + \frac{d_{31} w^{(2)}}{g^2(1+\alpha\varepsilon_0)}(A_{s1} e^{gz} - A_{s4} e^{-gz}) \tag{86}$$

For the mechanical governing equations of the laminated region ($L_1 < x < L_2$), based on the induced polarization in Eq. (85) and electro-mechanical coupling governing equations in Eqs. (37) and (38), the following equations are derived as

$$a_{i3} \cdot w^{(4)} + a_{i6} \cdot w^{(6)} + a_5 \cdot u_0^{(5)} + T_{i4} \cdot u_0^{(4)} + a_{i7} \cdot u_0^{(3)} = q \tag{87}$$

$$a_{i2} \cdot w^{(3)} + T_{i10} \cdot w^{(4)} + a_{i8} \cdot w^{(5)} + a_{i4} \cdot u_0^{(4)} + a_{i1} \cdot u_0^{(2)} = 0 \tag{88}$$

Similarly, according to the induced polarization in Eq. (85) and electro-mechanical coupling boundary conditions in Eqs. (41)–(45), the mechanical boundary conditions of the laminated region ($L_1 < x < L_2$) are derived as

$$-a_{i3} \cdot w^{(3)} - a_{i6} \cdot w^{(5)} - a_{i5} \cdot u_0^{(4)} - T_{i4} \cdot u_0^{(3)} - a_{i7} \cdot u_0^{(2)} = V$$
$$or \quad w = \bar{w} \quad when \quad x = L_1 \quad and \quad x = L_2 \tag{89}$$

$$a_{i3} \cdot w^{(2)} + a_{i6} \cdot w^{(4)} + a_{i5} \cdot u_0^{(3)} + T_{i4} \cdot u_0^{(2)} + a_{i7} \cdot u_0^{(1)}$$
$$+ [\frac{-bV f_{3113}}{\alpha} + \frac{bV d_{31}(h_1+h_2)}{2\alpha}] = M \tag{90}$$
$$or \quad w^{(1)} = \bar{w}^{(1)} \quad when \quad x = L_1 \quad and \quad x = L_2$$

$$-a_{i6} \cdot w^{(3)} - a_{i5} \cdot u_0^{(2)} - T_{i6} \cdot w^{(2)} - T_{i7} \cdot u_0^{(1)}$$
$$+ \frac{bV f_{1113}(h_1+h_2)}{2\alpha} = M^h \tag{91}$$
$$or \quad w^{(2)} = \bar{w}^{(2)} \quad when \quad x = L_1 \quad and \quad x = L_2$$

$$-a_{i2} \cdot w^{(2)} - a_{i8} \cdot w^{(4)} - a_{i4} \cdot u_0^{(3)} - T_{i10} \cdot w^{(3)} - a_{i1} \cdot u_0^{(1)} + \frac{bV d_{31}}{\alpha} = 0$$
$$or \quad u_0 = \bar{u}_0 \quad when \quad x = L_1 \quad and \quad x = L_2 \tag{92}$$

$$a_{i8} \cdot w^{(3)} + a_{i4} \cdot u_0^{(2)} + T_{i13} \cdot w^{(2)} + T_{i14} \cdot u_0^{(1)} + \frac{bV f_{1113}}{\alpha} = 0$$
$$or \quad u_0^{(1)} = \bar{u}_0^{(1)} \quad when \quad x = L_1 \quad and \quad x = L_2 \tag{93}$$

Here, the parameters $a_n (n = 1, 2, \ldots, 7)$ in Eqs. (87)–(93) are defined as follows

$$a_{i1} = -A_1 + T_{i12} \quad a_{i2} = A_2 + T_{i8} \quad a_{i3} = A_3 + T_{i1} \quad a_{i4} = A_4 + T_{i11}$$
$$a_{i5} = A_5 + T_{i3} \quad a_{i6} = -A_6 + T_{i2} \quad a_{i7} = -A_2 + T_{i5} \quad a_{i8} = -A_5 + T_{i9} \tag{94}$$

For brevity, the parameters $T_{in} (n = 1, 2, \ldots, 14)$ in inverse electro-mechanical governing equations of Eqs. (87)–(88) and boundary conditions of Eqs. (89)–(94) are given in Appendix F.

From the comparison between the mechanical governing equation in the Eqs. (87) and (88) of the inverse electro-mechanical problem, and that in the Eqs. (66) and (67) of the direct electro-mechanical problem, the expression of the deflection and axial displacement solution for the laminated region ($L_1 < x < L_2$) of the direct/inverse electro-mechanical problem are similar. Moreover, the deflection solutions for the non-laminated region ($0 < x < L_1$, $L_2 < x < L$) of the inverse

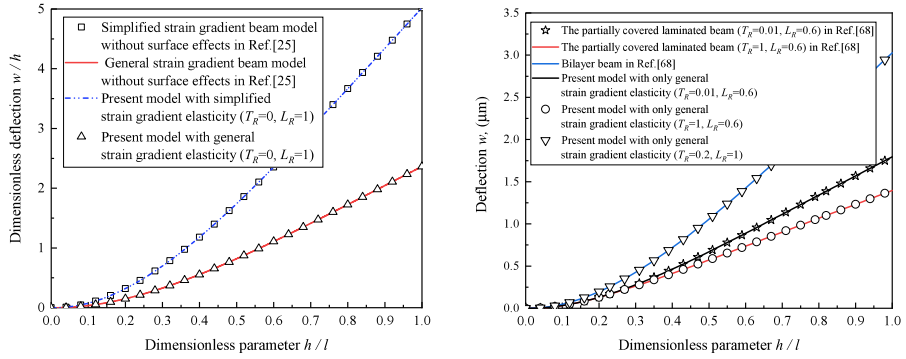

(a) Monolayer cantilever beam (b) Laminated cantilever beam

Fig. 2. The deflection comparison among the present model and existed models.

electro-mechanical problem are respectively similar to those of the direct electro-mechanical problem in the Eqs. (70) and (71).

The deflection and axial displacement induced from the inverse electro-mechanical problem can also be determined by using the equilibrium of forces conditions, the deformation compatibility conditions and the boundary conditions. For the equilibrium conditions of internal forces of the inverse electro-mechanical problem, the shear force is similar to those of the direct electro-mechanical problem in the Eqs. (72) while the classical moment and non-classical moment are different from that in the Eqs. (73) and (74) of the direct electro-mechanical problem. For the equilibrium conditions of classical moment at the conjunction, the following equations are given

$$\begin{aligned} &s \cdot w_2^{(2)}(L_1) - k \cdot w_2^{(4)}(L_1) = a_{i3} \cdot w_1^{(2)}(L_1) + a_{i6} \cdot w_1^{(4)}(L_1) \\ &+ a_{i5} \cdot u_0^{(3)}(L_1) + T_{i4} \cdot u_0^{(2)}(L_1) + a_{i7} \cdot u_0^{(1)}(L_1) \\ &+ [\frac{-bVf_{3113}}{\alpha} + \frac{bVd_{31}(h_1+h_2)}{2\alpha}] \\ &a_{i3} \cdot w_1^{(2)}(L_2) + a_{i6} \cdot w_1^{(4)}(L_2) + a_{i5} \cdot u_0^{(3)}(L_2) + T_{i4} \cdot u_0^{(2)}(L_2) \\ &+ a_{i7} \cdot u_0^{(1)}(L_2) + [\frac{-bVf_{3113}}{\alpha} + \frac{bVd_{31}(h_1+h_2)}{2\alpha}] \\ &= s \cdot w_3^{(2)}(L_2) - k \cdot w_3^{(4)}(L_2) \end{aligned} \tag{95}$$

For the equilibrium conditions of non-classical moment at the conjunction, the following equations are given

$$\begin{aligned} &k \cdot w_2^{(3)}(L_1) = -a_{i6} \cdot w_1^{(3)}(L_1) - a_{i5} \cdot u_0^{(2)}(L_1) - T_{i6} \cdot w_1^{(2)}(L_1) \\ &- T_{i7} \cdot u_0^{(1)}(L_1) + \frac{bVf_{1113}(h_1+h_2)}{2\alpha} \\ &- a_{i6} \cdot w_1^{(3)}(L_2) - a_{i5} \cdot u_0^{(2)}(L_2) - T_{i6} \cdot w_1^{(2)}(L_2) - T_{i7} \cdot u_0^{(1)}(L_2) \\ &+ \frac{bVf_{1113}(h_1+h_2)}{2\alpha} = k \cdot w_3^{(3)}(L_2) \end{aligned} \tag{96}$$

The deformation compatibility conditions at the conjunction of the direct and inverse electro-mechanical problem are the same and already shown in Eq. (75). The cantilever boundary conditions are also given in Eqs. (76).

Thus, according to the equilibrium of forces conditions, the deformation compatibility conditions and the cantilever boundary conditions, the deflection and axial displacement induced from the inverse electro-mechanical process is obtained. The inverse electro-mechanical response of the cantilever piezoelectric microbeam is determined. Similarly, the inverse electro-mechanical problem of the piezoelectric microbeam under other boundary conditions can also be solved.

6. Results and discussions

The size-dependent electro-mechanical analysis of the piezoelectric microbeam is performed. The material of lower beam is silicon. The material parameters are E_1= 130 Gpa. ν_1= 0.35. The geometric parameters

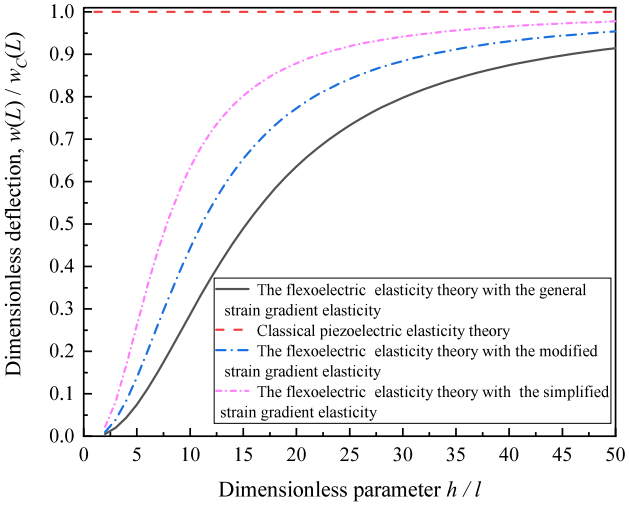

Fig. 3. Size effects of the deflection of the cantilever beam with T_R = 0.2, L_R = 0.6 and $L_1 + L_2 = L$.

satisfy: $L = 25h_1$, $b_1 = 2h_1$. The material of upper beam is $BaTio_3$. The material parameters are c_{11} = 131 Gpa. ν_2 = 0.3, $\epsilon_0 = 8.85\times10^{-15}$ F/ μm, $\alpha_{33} = 0.79\times10^8$ V m/C, $b_{33} = 1\times10^{-9}$ J m^3/C^2, $d_{31} = 1.87\times10^8$ V/m [66]. The flexoelectric coefficients are $f_{1113} = f_{3311} = f_{3113} = 5V$ [3]. The thickness of upper layer is h_2. The width of upper layer satisfies: $b_2 = b_1$. The total thickness of the beam is $h = h_1 + h_2$. We define T_R as the thickness ratio, $T_R = h_2/h_1$. L_R is defined as the length ratio, $L_R = (L_2 - L_1)/L$. In addition, the length parameters satisfy: $l_{i(1)} = l$, $l_{i(2)} = 0.5l (i = 0, 1, 2)$, l = 0.428 μm [68]. The uniformly distributed load q = 10 μN/m. The external voltage is V = 20 V.

The deflection of present model with different strain gradient elasticity and laminated region geometric parameters is shown in Fig. 2. From the figure, it can be seen that the present model with only the general or simplified strain gradient elasticity can respectively reduce to the general or simplified strain gradient monolayer beam model without surface effects in Ref. [25] when the laminated region geometric parameters satisfy $T_R = 0$, $L_R = 1$. Moreover, when the laminated region geometric parameters satisfy $T_R = 1$, $L_R = 0.6$, by ignoring the electric elasticity, the present model with only general strain gradient elasticity reduces to the elastic partially covered laminated beam model in Ref. [68]. When the laminated region geometric parameters satisfy $T_R = 0.2$, $L_R = 1$, the present model without electric elasticity reduces to the general strain gradient bilayer beam model in Ref. [68].

The comparison of the deflection of the non-classical model and classical model is shown in Fig. 3. $w(L)$ is the deflection of the non-classical model. $w_c(L)$ is the deflection of the classical model. It can be

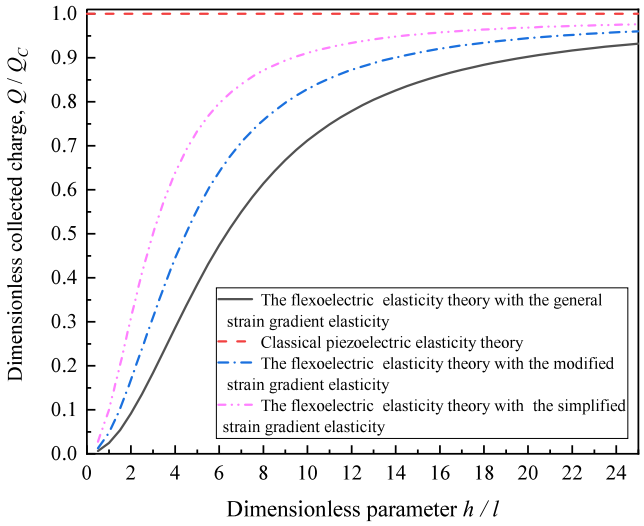

Fig. 4. Size effects of the collected charge of the cantilever beam with $T_R = 0.2$, $L_R = 0.6$ and $L_1 + L_2 = L$.

seen that the deflections of the non-classical models decrease gradually with the decrease of the ratio of the thickness and the length parameters, and thus show size dependency obviously. However, the deflection of the classical model is independent of the ratio. The flexoelectric elasticity theories with the strain gradient elasticity can describe the size-dependent behaviour of the deflection while the classical piezoelectric elasticity theory fails to explain the size effects. Moreover, compared with the flexoelectric elasticity theory with the general strain gradient elasticity, the simplified flexoelectric elasticity theories with the approximated strain gradient elasticity predict larger deflection. The simplified flexoelectric elasticity theories include only part of strain gradients and thus underestimate the size effects.

The collected charge induced from the direct electro-mechanical process is shown in Fig. 4. Q is the collected charge of the non-classical model. Q_c is the collected charge of the classical model. From the figure, the collected charge of the non-classical model is dependent on the ratio of the thickness and the length parameters, and varies with the ratio. However, the collected charge of the classical model is independent of the ratio. The limitations of the classical model is thus revealed. In addition, it can be seen that the collected charge of the flexoelectric elasticity theory with the general strain gradient elasticity is much smaller than that of the simplified flexoelectric elasticity theories with the modified or simplified strain gradient elasticity. Compared with the general strain gradient elasticity, the modified or simplified strain gradient elasticity includes only part of strain gradients. The simplified strain gradient elasticity has less strain gradients than that of the modified strain gradient elasticity. The bending stiffness of the beam with the modified strain gradient elasticity is largest while the collected charge induced from the bending process is smallest. The flexoelectric elasticity theory with the general strain gradient elasticity includes all strain gradients and thus can reflect the size effects more appropriately.

The polarization and electric potential induced from the direct electro-mechanical process are respectively shown in Fig. 5. $\xi = (z + h_2 + \frac{1}{2}h_1)/h_2$ is the dimensionless thickness. $\xi = 0$ is the upper surface. $\xi = 1$ is the lower surface. The polarization and electric potential distribute non-uniformly along the thickness direction. The polarization varies obviously when the dimensionless parameter ξ closes to the surface of the piezoelectric layer while the electric potential decreases along most part of the thickness. The direction of the electric potential changes due to the combined effects of the flexoelectricity and piezoelectricity. Moreover, compared with the flexoelectric elasticity theory with the general strain gradient elasticity, the polarization and electric potential of the flexoelectric elasticity theories with the modified or simplified strain gradient elasticity are larger. Due to contain only part of strain gradients, the bending stiffness of the microbeam of the modified or simplified theories is smaller, the beam undergoes larger bending deformation and produces stronger polarization and electric potential. Compared with the flexoelectric elasticity theory with the modified strain gradient elasticity, the polarization and electric potential of the flexoelectric elasticity theory with the general or simplified strain gradient elasticity is smaller or larger. Therefore, the simplified flexoelectric elasticity theories with the approximated strain gradient elasticity underestimate the size-dependent direct electro-mechanical process.

The size effects of the induced polarization is shown in Fig. 6. $\xi = (z + h_2 + \frac{1}{2}h_1)/h_2$ is the dimensionless thickness. $\xi = 0$ is the upper surface. $\xi = 1$ is the lower surface. The polarization increases gradually with the increase of the dimensionless thickness h/l, depends on the dimensionless thickness h/l and thus exhibits size dependency. When the dimensionless thickness h/l decreases, the effects from strain gradient become obvious, the beam bending rigidity increases, the bending deformation decreases, and thus the quantity of the induced polarization decreases. When the dimensionless thickness h/l increases, the effects from strain gradient become weak, the beam bending rigidity decreases and the bending deformation increases, and thus the quantity of the induced polarization increases. As shown in Fig. 5a, when the dimensionless parameter ξ satisfies $\xi = 0.5$, the dimensionless thickness h/l increases from 0.1 to 2, the induced polarization almost increases by two times. In addition, it can be seen that the induced polarization distributes non-uniformly along the thickness direction. When the dimensionless parameter ξ satisfies $0 < \xi < 0.1$ or $0.9 < \xi < 1$, the induced polarization varies obviously. When the dimensionless parameter ξ satisfies $0.1 < \xi < 0.9$, the induced polarization varies slowly.

The effects of strain gradient elasticity and flexoelectricity on the polarization induced from the direct electro-mechanical process are

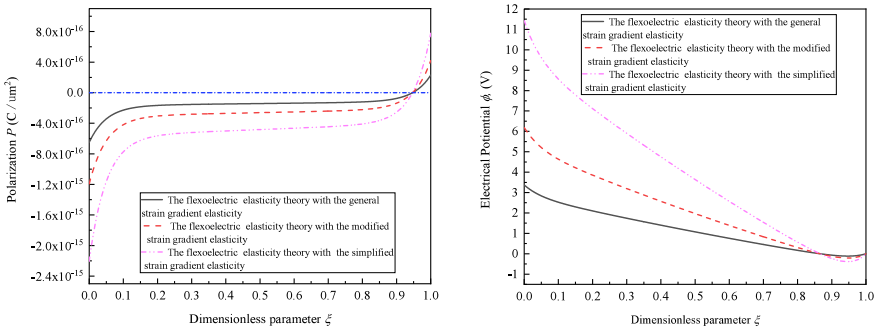

Fig. 5. The polarization and electric potential at the midpoint of the cantilever beam induced from the direct electro-mechanical process with $T_R = 0.2$, $h_1 = 1$ μm, $L_R = 0.6$ and $L_1 + L_2 = L$.

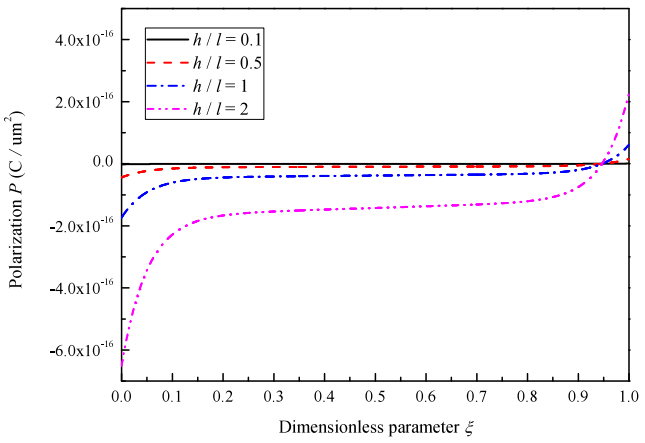

Fig. 6. Size effects of the polarization at the midpoint of the cantilever beam with $T_R = 0.2$, $L_R = 0.6$ and $L_1 + L_2 = L$.

shown in Fig. 7. $\xi = (z + h_2 + \frac{1}{2}h_1)/h_2$ is the dimensionless thickness. $\xi = 0$ is the upper surface. $\xi = 1$ is the lower surface. The polarization induced from the piezoelectricity decreases slightly along the thickness direction. However, the polarization induced from the flexoelectricity varies obviously when the dimensionless parameter ξ closes to the surface of the piezoelectric layer. The flexoelectricity affects the polarization greatly and enhances the polarization of the surface of the piezoelectric layer. Moreover, the effects from the strain gradient elasticity on the induced polarization are significant. The inclusion of strain gradient elasticity enhances the bending rigidity, weakens the bending deformation, and reduces the induced polarization. As shown in Figs. 6a and 6b, when the dimensionless parameter ξ is $\xi = 0.5$, the induced polarization from the flexoelectricity and piezoelectricity with strain gradient elasticity is almost 2% of that without the strain gradient elasticity. Therefore, the strain gradient elasticity should be considered to appropriately describe the size dependency of the induced polarization.

The size dependency of the electric potential induced from the direct electro-mechanical process is shown in Fig. 8. $\xi = (z+h_2+\frac{1}{2}h_1)/h_2$ is the dimensionless thickness. $\xi = 0$ is the upper surface. $\xi = 1$ is the lower surface. The electric potential decreases gradually with the decrease of the dimensionless thickness h/l, depends on the dimensionless thickness h/l and shows size dependency. When the dimensionless thickness h/l increases, the strain gradient effects decreases, the bending rigidity decreases, and thus the induced electric potential increases. When the dimensionless thickness h/l decreases, the strain gradient effects increases, the bending rigidity increases, and thus the induced electric potential decreases. As shown in Fig. 7a, when the dimensionless thickness is $\xi = 0$, the dimensionless thickness h/l increases from 5 to 10, the induced electric potential has almost increased by 2.4 times. Moreover, it can be seen that the induced electric potential decreases gradually along the most part of the thickness. However, when the dimensionless parameter ξ closes to the bottom surface of the piezoelectric layer, the direction of the induced electric potential changes. The variation of the direction of the induced electric potential is the results of the superposition of the piezoelectricity and flexoelectricity.

The influence of strain gradient elasticity and flexoelectricity on the induced electric potential is shown in Fig. 9. $\xi = (z + h_2 + \frac{1}{2}h_1)/h_2$ is the dimensionless thickness. $\xi = 0$ is the upper surface. $\xi = 1$ is the lower surface. From the figure, it can be seen that the variation law of the electric potential respectively induced from the piezoelectricity and flexoelectricity along the dimensionless thickness is different. The induced electric potential from the piezoelectricity decreases constantly along the dimensionless thickness. However, the electric potential induced from the flexoelectricity increases gradually when the dimensionless parameter ξ satisfies $0 < \xi < 0.1$, and then decreases along the dimensionless thickness. The electric potential induced from the piezoelectricity is much larger than that induced from the flexoelectricity and piezoelectricity. Namely, the flexoelectricity weakens the electric potential of the piezoelectric microbeam. Moreover, the induced electric potential is highly affected by strain gradient elasticity. When the strain gradient elasticity is considered, the bending deformation is weakened and thus the induced electric potential becomes smaller. As shown in Figs. 8a and 8b, when the dimensionless parameter ξ is $\xi = 0.5$, the induced electric potential from the flexoelectricity and piezoelectricity with strain gradient elasticity is almost 2% of that without the strain gradient elasticity. Thus, the strain gradient elasticity should be included to estimate the size-dependent response of the induced electric potential.

The bending deformation induced from the inverse electro-mechanical process is shown in Fig. 10. It can be seen that the induced deflections from the simplified flexoelectric elasticity theories with the approximated strain gradient elasticity are much larger than that from the flexoelectric elasticity theory with the general strain gradient elasticity. As shown in Fig. 9a, when the dimensionless length is $x/L = 1$, the deflection induced from the flexoelectric elasticity theory with the simplified strain gradient elasticity and the flexoelectric elasticity theory with the modified strain gradient elasticity is almost 3.5 times and 2 times than that from the flexoelectric elasticity theory with the general strain gradient elasticity, respectively. This implies that compared with the general theory, the simplified theories with only part of the strain gradients underestimate the size-dependent inverse electro-mechanical response.

The deflection of the piezoelectric microbeam induced from the different inverse electro-mechanical mechanism is shown in Fig. 11. It can be seen that the deflection induced from the inverse piezoelectric mechanism is much larger than that from the inverse flexoelectric mechanism. As shown in Fig. 10a, when the dimensionless length is $x/L = 1$, the deflection induced from the piezoelectricity is almost 20 times than that from the flexoelectricity. In addition, it should be noted that the induced deflection from the piezoelectricity is almost same as that from the piezoelectricity and flexoelectricity. This implies

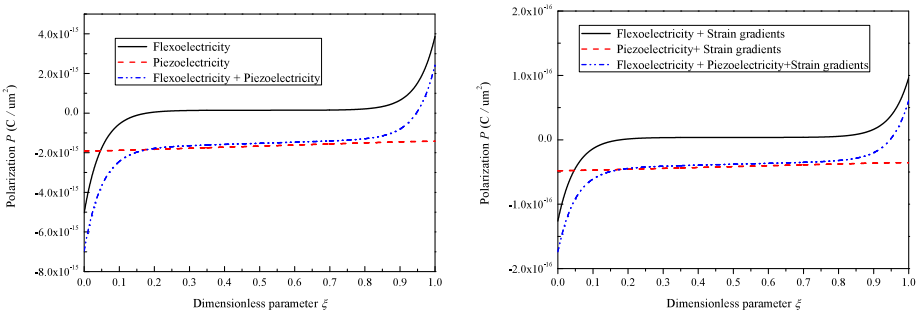

Fig. 7. Influence of the strain gradient elasticity and flexoelectricity on the polarization at the midpoint of the cantilever beam with $T_R = 0.2$, $h_1 = 1$ μm, $L_R = 0.6$ and $L_1 + L_2 = L$.

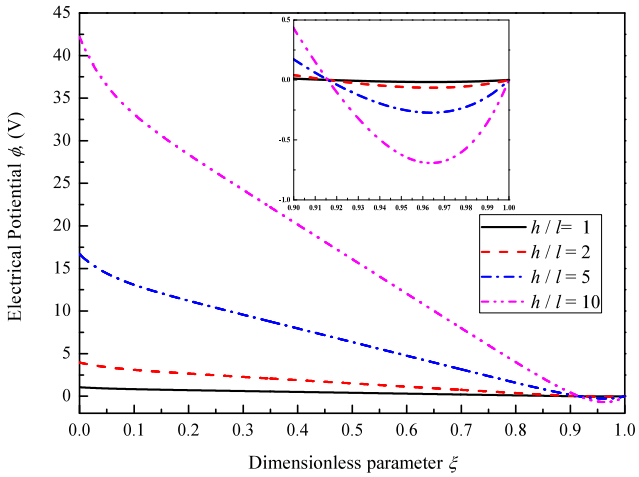

Fig. 8. Size effects of the electric potential at the midpoint of the cantilever beam with $T_R = 0.2$, $L_R = 0.6$ and $L_1 + L_2 = L$.

that compared with the flexoelectricity, the piezoelectricity is predominant on the inverse electro-mechanical process of the piezoelectric microbeam when the beam thickness is in micron range.

The size effects of the deflection induced from the inverse electro-mechanical process is shown in Fig. 12. $w(L)$ is the deflection of the non-classical model. $w_c(L)$ is the deflection of the classical model. As the decrease of the ratio of the thickness and the length parameters, the dimensionless deflection decreases gradually, thus shows size dependency obviously. When the ratio is small enough, the dimensionless deflection of the non-classical model is much smaller than that of the classical model. When the ratio is large enough, the dimensionless deflection of the non-classical model is constant and independent of the variation of the ratio. The effectiveness of the non-classical model and the limitation of the classical model is simultaneously revealed via the inverse electro-mechanical problem.

The bending direction of the piezoelectric microbeam under different external voltage is shown in Fig. 13. The direction of the deflection induced from the inverse electro-mechanical process is dependent on the positive or negative of the external voltage. When the external voltage is applied at the surface layer of the piezoelectric layer, due to the inverse piezoelectric/flexoelectric process, the equivalent bending moment will produce at the ends of the piezoelectric layer. From the classical moment equilibrium conditions in Eqs. (95), it can seen that the equivalent bending moments induced from the inverse flexoelectric process and inverse piezoelectric process are bVf_{3113}/α and $bVd_{31}(h_1+h_2)/2\alpha$, respectively. The positive or negative of the external voltage affects the direction of the equivalent bending moment, and thus determines the bending direction of the beam. For a cantilever piezoelectric microbeam, if the external voltage is positive, then the negative equivalent bending moment is generated at the ends of the piezoelectric layer, and makes the beam bend downward. When the external voltage is negative, then the positive equivalent bending moment is generated at the ends of the piezoelectric layer, and makes the beam bend upward.

7. Conclusions

In this paper, the general strain gradient elasticity with three independent material length-scale parameters is incorporated into the flexoelectric elasticity theory. The degeneration analysis of the flexoelectric elasticity theory with the general strain gradient elasticity is performed. By neglecting some strain gradients, the flexoelectric elasticity theory with the general strain gradient elasticity can reduce to the simplified flexoelectric elasticity theory with the approximated strain gradient elasticity including the modified strain gradient elasticity and the simplified strain gradient elasticity. Subsequently, the direct/inverse electro-mechanical analysis of the laminated microbeam with a partially covered piezoelectric layer under the uniformly distributed load and external voltage is performed.

For the direct electro-mechanical analysis, the collected charge, the polarization, the electric potential increase with the increase of the ratio of the thickness and length parameters, and show size dependency apparently. Compared with the general theory, the simplified theories predict larger collected charge, polarization and electric potential, and underestimate the direct electro-mechanical response. The polarization induced from the piezoelectricity decreases slowly along the thickness direction while the polarization induced from the flexoelectricity decreases obviously at the surface of the piezoelectric layer. The electric potential induced from the piezoelectricity decreases more obvious than that induced from the flexoelectricity. The flexoelectricity enhances the polarization while weakens the electric potential of the piezoelectric microbem. For the inverse electro-mechanical analysis, the deflection relies on the ratio of the thickness and length parameters, and decreases with the decrease of the ratio. Compared with the general theory, the simplified theories predict larger deflection, and underestimate the inverse electro-mechanical response. The deflection induced from the piezoelectricity is larger than that from the flexoelectricity. The flexoelectricity along hardly affects the deflection of the piezoelectric microbem when the thickness is in micron range. Moreover, the strain gradient elasticity greatly weakens the direct/inverse electro-mechanical response when the thickness is comparable to the material length-scale parameters. The limitations of this study include the ideal interface contact conditions and the simple geometry. In the future, we will devote to study the more complicated case that the multiphysics field response of the laminated structure with a partially covered smart layer under the imperfect interface contact conditions. We hope a more firm conclusions can be formulated and offer theoretical basis for the design of the partially covered laminated structure-based microdevice.

CRediT authorship contribution statement

Guangyang Fu: Methodology, Formal analysis, Writing – original draft. **Zhenjie Zhang:** Methodology, Review. **Chunmei Dong:** Review. **Guangxi Zhao:** Software, Calculation. **Jianjun Wang:** Conceptualization, Resources, Writing – review & editing, Funding acquisition. **Xuye Zhuang:** Conceptualization, Resources, Writing – review & editing, Funding acquisition. **Hongyu Zheng:** Conceptualization, Resources, Writing – review & editing, Funding acquisition.

Declaration of competing interest

The authors declare that they have no known competing financial interests or personal relationships that could have appeared to influence the work reported in this paper.

Data availability

No data was used for the research described in the article.

Acknowledgments

This work was supported by the National Key R & D Program (2022YFB4600402), Natural Science Foundation of Shandong Province of China (ZR2021QA078), Taishan Scholars Program of Shandong Province (ts20190401, tsqn201909108), the Natural Science Foundation of Shandong Province of China (ZR2020ME164, ZR2021MF042), the Key Research and Development Project of Zibo City (2020SNPT0088, 2021SNCG0053), the School-city Integration Project in Zhangdian District (2021JSCG0020), the Open Fund of State Key Laboratory of Applied Optics (SKLAO2020001A16) and the Shandong Provincial Key Laboratory of Precision Manufacturing and Non-traditional Machining. and Shandong Province science and technology smes innovation ability improvement project (2022TSGC2278)

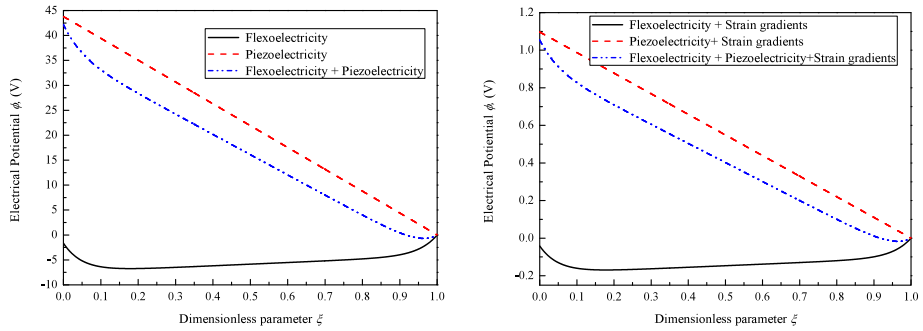

Fig. 9. Influence of the strain gradient elasticity and flexoelectricity on the electric potential induced from the direct electro-mechanical problem at the midpoint of the cantilever beam with $T_R = 0.2$, $h_1 = 1$ μm, $L_R = 0.6$ and $L_1 + L_2 = L$.

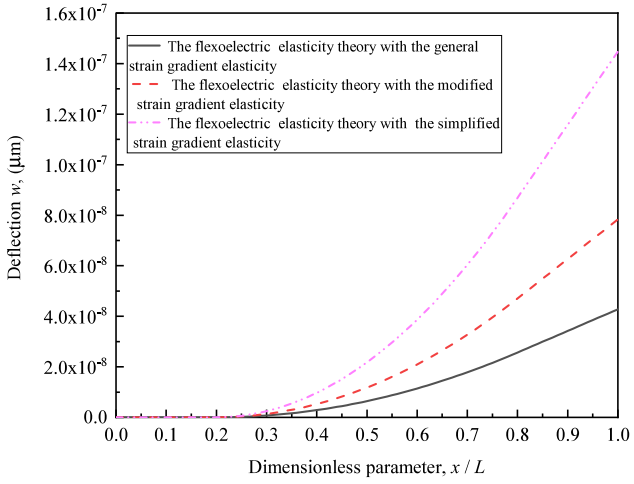

Fig. 10. The deflection of the cantilever beam induced from the inverse electro-mechanical process with $T_R = 0.2$, $h_1 = 1$ μm, $L_R = 0.6$ and $L_1 + L_2 = L$.

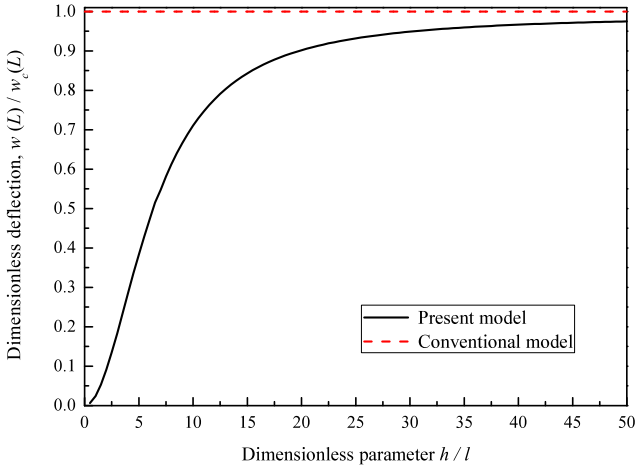

Fig. 12. Size effects of the induced deflection of the cantilever beam with $T_R = 0.2$, $L_R = 0.6$ and $L_1 + L_2 = L$.

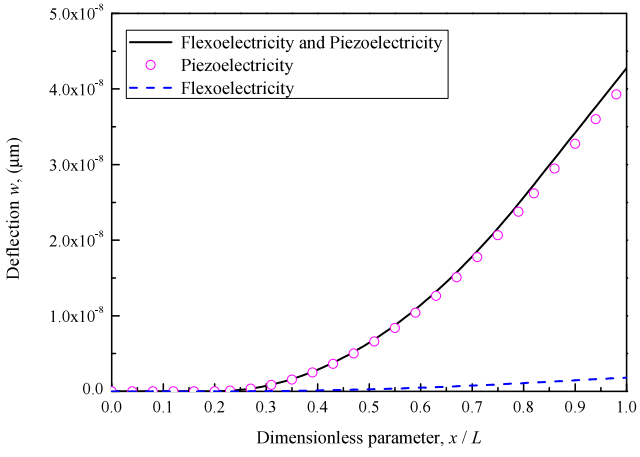

Fig. 11. Influence of the flexoelectricity and piezoelectricity on the induced deflection of the cantilever beam with $T_R = 0.2$, $h_1 = 1$ μm, $L_R = 0.6$ and $L_1 + L_2 = L$.

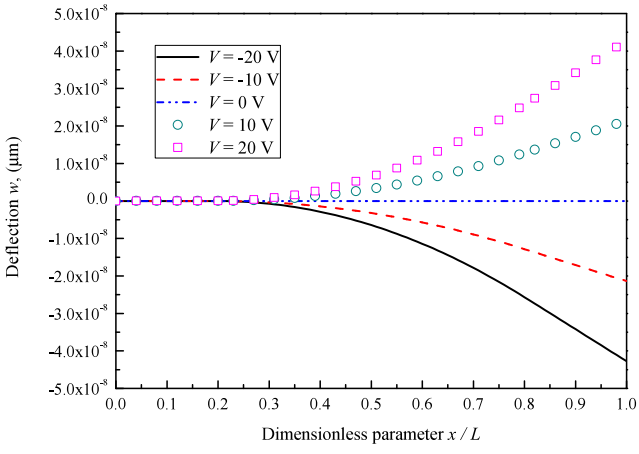

Fig. 13. The bending direction of the cantilever beam under different external voltage with $T_R = 0.2$, $h_1 = 1$ μm, $L_R = 0.6$ and $L_1 + L_2 = L$.

Appendix A

The formulation of the laminated region ($L_1 < x < L_2$) after the variation are shown as follows

$$\begin{aligned}
&\int_{L_1}^{L_2}[A_3\cdot w^{(4)}-A_6\cdot w^{(6)}+A_5\cdot u_0^{(5)}-A_2\cdot u_0^{(3)}+\int_{A_{(2)}}[-f_{3113}\frac{d^2P_3}{dx^2}\\
&+f_{3311}z\frac{d^3P_3}{dx^2dz}+f_{1113}\frac{d^3P_3}{dx^3}z-d_{113}z\frac{d^2P_3}{dx^2}]dA_{(2)}-q(x)]\delta w dx\\
&+[-A_3\cdot w^{(3)}+A_6\cdot w^{(5)}-A_5\cdot u_0^{(4)}+A_2\cdot u_0^{(2)}+\int_{A_{(2)}}[f_{3113}\frac{dP_3}{dx}\\
&-f_{3311}z\frac{d^2P_3}{dxdz}-f_{1113}\frac{d^2P_3}{dx^2}z+d_{113}z\frac{dP_3}{dx}]dA_{(2)}-V]\delta w|_{L_1}^{L_2}+[A_3\cdot w^{(2)}\\
&-A_6\cdot w^{(4)}+A_5\cdot u_0^{(3)}-A_2\cdot u_0^{(1)}+\int_{A_{(2)}}[-f_{3113}P_3+f_{3311}z\frac{dP_3}{dz}\\
&+f_{1113}\frac{dP_3}{dx}z-d_{113}zP_3]dA_{(2)}-M]\delta w^{(1)}|_{L_1}^{L_2}+[A_6\cdot w^{(3)}-A_5\cdot u_0^{(2)}\\
&-f_{1113}zP_3-M^h]\delta w^{(2)}|_{L_1}^{L_2}+\int_0^{L_1}[A_2\cdot w^{(3)}-A_5\cdot w^{(5)}+A_4\cdot u_0^{(4)}\\
&-A_1\cdot u_0^{(2)}+\int_{A_{(2)}}[f_{1113}\frac{d^2P_3}{dx^2}+f_{3311}\frac{d^2P_3}{dxdz}-d_{113}\frac{dP_3}{dx}]dA_{(2)}]\delta u_0 dx\\
&+[-A_2\cdot w^{(2)}+A_5\cdot w^{(4)}-A_4\cdot u_0^{(3)}+A_1\cdot u_0^{(1)}+\int_{A_{(2)}}[-f_{1113}\frac{dP_3}{dx}\\
&-f_{3311}\frac{dP_3}{dz}+d_{113}P_3]dA_{(2)}]\delta u_0|_{L_1}^{L_2}+[-A_5\cdot w^{(3)}+A_4\cdot u_0^{(2)}+f_{1113}P_3\\
&]\delta u_0^{(1)}|_{L_1}^{L_2}+b\int_0^{L_1}\int_{-(h_2+\frac{h_1}{2})}^{-\frac{h_1}{2}}[\alpha P_3-b_{33}\frac{d^2P_3}{dz^2}+f_{1113}(u_0^{(2)}-zw^{(3)})\\
&-f_{3113}w^{(2)}-f_{3311}w^{(2)}+\frac{d\varphi}{dz}+d_{113}(u_0^{(1)}-zw^{(2)})]\delta P_3 dzdx\\
&+b\int_{L_1}^{L_2}\int_{-(h_2+\frac{h_1}{2})}^{-\frac{h_1}{2}}[-\varepsilon_0\frac{d^2\varphi}{dz^2}+\frac{dP_3}{dz}]\delta\varphi_3 dzdx+[b_{33}\frac{dP_3}{dz}+f_{3311}zw^{(2)}\\
&-f_{3311}u_0^{(1)}]\delta P_3|_{-(h_2+\frac{h_1}{2})}^{-\frac{h_1}{2}}+[-\varepsilon_0\frac{d\varphi}{dz}+P_3]\delta\varphi_3|_{-(h_2+\frac{h_1}{2})}^{-\frac{h_1}{2}}=0
\end{aligned}\tag{A.1}$$

Appendix B

The unknown constants $c_n(n=1,2,3,4,5)$ in the Eqs. (52) and (53) are determined as follows

$$A_s=e^{g(h_2-\frac{h_1}{2})}-e^{-g(h_2+\frac{h_1}{2})}\tag{B.1}$$

$$B_s=e^{g(h_2+\frac{h_1}{2})}-e^{g(\frac{h_1}{2}-h_2)}\tag{B.2}$$

$$c_{1f}=\frac{2f_{3113}\varepsilon_0}{(1+\alpha\varepsilon_0)}w^{(2)}-\frac{f_{1113}\varepsilon_0}{(1+\alpha\varepsilon_0)}u_0^{(2)}\tag{B.3}$$

$$c_{1p}=-\frac{d_{31}\varepsilon_0}{(1+\alpha\varepsilon_0)}u_0^{(1)}\tag{B.4}$$

$$\begin{aligned}
c_{2f}=&\frac{f_{1113}\varepsilon_0}{g(1+\alpha\varepsilon_0)}(1-e^{gh_2})A_sw^{(3)}+\frac{\frac{h_1}{2}f_{3311}g\varepsilon_0}{(1+\alpha\varepsilon_0)}e^{gh_2}A_sw^{(2)}\\
&-\frac{(h_2+\frac{h_1}{2})f_{3311}g\varepsilon_0}{(1+\alpha\varepsilon_0)}A_sw^{(2)}+\frac{f_{3311}g\varepsilon_0}{(1+\alpha\varepsilon_0)}(e^{gh_2}-1)A_su_0^{(1)}
\end{aligned}\tag{B.5}$$

$$c_{2p}=\frac{d_{31}\varepsilon_0}{g(1+\alpha\varepsilon_0)}(1-e^{gh_2})A_sw^{(2)}\tag{B.6}$$

$$\begin{aligned}
c_{3f}=&\frac{f_{1113}\varepsilon_0}{g(1+\alpha\varepsilon_0)}(1-e^{-gh_2})B_sw^{(3)}+\frac{\frac{h_1}{2}f_{3311}g\varepsilon_0}{(1+\alpha\varepsilon_0)}e^{-gh_2}B_sw^{(2)}\\
&-\frac{(h_2+\frac{h_1}{2})f_{3311}g\varepsilon_0}{(1+\alpha\varepsilon_0)}B_sw^{(2)}+\frac{f_{3311}g\varepsilon_0}{(1+\alpha\varepsilon_0)}(e^{-gh_2}-1)B_su_0^{(1)}
\end{aligned}\tag{B.7}$$

$$c_{3p}=\frac{d_{31}\varepsilon_0}{g(1+\alpha\varepsilon_0)}(1-e^{-gh_2})B_sw^{(2)}\tag{B.8}$$

$$\begin{aligned}
c_{4f}=&\frac{f_{1113}b_{33}\varepsilon_0}{(1+\alpha\varepsilon_0)^2}w^{(3)}-\frac{f_{1113}h_1^2}{8(1+\alpha\varepsilon_0)}w^{(3)}+\frac{f_{3311}\frac{h_1}{2}}{(1+\alpha\varepsilon_0)}w^{(2)}\\
&-\frac{f_{1113}\frac{h_1}{2}}{(1+\alpha\varepsilon_0)}u_0^{(2)}-\frac{f_{3311}}{(1+\alpha\varepsilon_0)}u_0^{(1)}
\end{aligned}\tag{B.9}$$

$$c_{4p}=\frac{d_{31}b_{33}\varepsilon_0}{(1+\alpha\varepsilon_0)^2}w^{(2)}-\frac{d_{31}h_1^2}{8(1+\alpha\varepsilon_0)}w^{(2)}-\frac{\frac{h_1}{2}d_{31}}{(1+\alpha\varepsilon_0)}u_0^{(1)}\tag{B.10}$$

$$c_{5f}=\frac{2f_{3113}}{(1+\alpha\varepsilon_0)}w^{(2)}-\frac{f_{1113}}{(1+\alpha\varepsilon_0)}u_0^{(2)}\tag{B.11}$$

$$c_{5p}=-\frac{d_{31}}{(1+\alpha\varepsilon_0)}u_0^{(1)}\tag{B.12}$$

The unknown constants $c_n(n=1,2,3,4,5)$ are determined as

$$\begin{aligned}
&c_1=c_{1f}+c_{1p}\quad c_2=c_{2f}+c_{2p}\quad c_3=c_{3f}+c_{3p}\\
&c_4=c_{4f}+c_{4p}\quad c_5=c_{5f}+c_{5p}
\end{aligned}\tag{B.13}$$

Here, c_{if} and $c_{ip}(i=1,2,3,4,5)$ are respectively the coefficients associated with the flexoelectric effects and piezoelectric effects.

Appendix C

The parameters $T_n(n=1,2,\ldots,14)$ in direct electro-mechanical governing equations of Eqs. (58)–(59) and boundary conditions of Eqs. (60)–(65) are given as follows.

$$\begin{aligned}
T_1=&\frac{bf_{3311}^2g\varepsilon_0h_1(h_2+\frac{h_1}{2})}{(1+\alpha\varepsilon_0)}A_{s7}+\frac{bf_{3311}^2g\varepsilon_0(h_2^2+h_1h_2+\frac{h_1^2}{2})}{(1+\alpha\varepsilon_0)}A_{s8}\\
&+(\frac{bf_{3311}d_{31}\varepsilon_0(h_2+h_1)}{g(1+\alpha\varepsilon_0)}-\frac{bd_{31}^2\varepsilon_0}{g^3(1+\alpha\varepsilon_0)})A_{s9}+\frac{bd_{31}^2h_2\varepsilon_0}{g^2(1+\alpha\varepsilon_0)}\\
&+\frac{bd_{31}^2\varepsilon_0}{(1+\alpha\varepsilon_0)}[\frac{-h_1^3}{24}+\frac{(h_2+\frac{1}{2}h_1)^3}{3}]
\end{aligned}\tag{C.1}$$

$$\begin{aligned}
T_2=&-\frac{bf_{1113}^2h_2\varepsilon_0}{g^2(1+\alpha\varepsilon_0)}+\frac{bf_{1113}^2\varepsilon_0}{(1+\alpha\varepsilon_0)}[\frac{-h_1^3}{24}+\frac{(h_2+\frac{1}{2}h_1)^3}{3}]\\
&+\frac{bf_{1113}^2\varepsilon_0}{g^3(1+\alpha\varepsilon_0)}A_{s9}
\end{aligned}\tag{C.2}$$

$$T_3=\frac{bf_{1113}^2h_2\varepsilon_0(h_2+h_1)}{2(1+\alpha\varepsilon_0)}\tag{C.3}$$

$$T_4=\frac{2bf_{1113}f_{3113}\varepsilon_0h_2}{(1+\alpha\varepsilon_0)}-\frac{bf_{1113}f_{3311}\varepsilon_0}{g(1+\alpha\varepsilon_0)}A_{s9}\tag{C.4}$$

$$\begin{aligned}
T_5=&-\frac{1}{2}\frac{bgf_{3311}^2\varepsilon_0(h_2+h_1)}{(1+\alpha\varepsilon_0)}A_{s9}-\frac{bd_{31}^2\varepsilon_0h_2(h_2+h_1)}{2(1+\alpha\varepsilon_0)}\\
&-\frac{bf_{3311}\varepsilon_0d_{31}}{g(1+\alpha\varepsilon_0)}A_{s9}
\end{aligned}\tag{C.5}$$

$$\begin{aligned}
T_6=&(-\frac{1}{2}\frac{bf_{3311}f_{1113}\varepsilon_0(h_2+h_1)}{g(1+\alpha\varepsilon_0)}+\frac{bd_{31}f_{1113}\varepsilon_0}{g^3(1+\alpha\varepsilon_0)})A_{s9}-\frac{bd_{31}f_{1113}h_2\varepsilon_0}{g^2(1+\alpha\varepsilon_0)}\\
&+\frac{bd_{31}f_{1113}\varepsilon_0}{(1+\alpha\varepsilon_0)}[\frac{-h_1^3}{24}+\frac{(h_2+\frac{1}{2}h_1)^3}{3}]
\end{aligned}\tag{C.6}$$

$$T_7=\frac{bf_{1113}d_{31}\varepsilon_0h_2(h_1+h_2)}{2(1+\alpha\varepsilon_0)}+\frac{bf_{1113}f_{3311}\varepsilon_0h_2}{(1+\alpha\varepsilon_0)}-\frac{bf_{1113}f_{3311}\varepsilon_0}{g(1+\alpha\varepsilon_0)}A_{s9}\tag{C.7}$$

$$T_8=(\frac{1}{2}\frac{bgf_{3311}^2\varepsilon_0(h_2+h_1)}{(1+\alpha\varepsilon_0)}-\frac{bd_{31}f_{3311}\varepsilon_0}{g(1+\alpha\varepsilon_0)})A_{s9}+\frac{bd_{31}^2\varepsilon_0h_2(h_2+h_1)}{2(1+\alpha\varepsilon_0)}\tag{C.8}$$

$$T_9=-\frac{bf_{1113}^2\varepsilon_0h_2(h_2+h_1)}{2(1+\alpha\varepsilon_0)}\tag{C.9}$$

$$T_{10} = \frac{2bf_{1113}f_{3311}\varepsilon_0 h_2}{(1+\alpha\varepsilon_0)} - \frac{bf_{1113}f_{3311}\varepsilon_0}{g(1+\alpha\varepsilon_0)}A_{s9} \tag{C.10}$$

$$T_{11} = -\frac{bf_{1113}^2\varepsilon_0 h_2}{(1+\alpha\varepsilon_0)} \tag{C.11}$$

$$T_{12} = \frac{bgf_{3311}^2\varepsilon_0}{(1+\alpha\varepsilon_0)}A_{s9} + \frac{bd_{31}^2\varepsilon_0 h_2}{(1+\alpha\varepsilon_0)} \tag{C.12}$$

$$T_{13} = \frac{bf_{3311}f_{1113}\varepsilon_0 h_2}{(1+\alpha\varepsilon_0)} - \frac{bd_{31}f_{1113}\varepsilon_0 h_2(h_2+h_1)}{2(1+\alpha\varepsilon_0)} \tag{C.13}$$

$$T_{14} = -\frac{bd_{31}f_{1113}\varepsilon_0 h_2}{(1+\alpha\varepsilon_0)} \tag{C.14}$$

In Eqs. (C.1)–(C.2), (C.4)–(C.8), (C.10) and (C.12), the parameters $A_{sn}(n=7,8,9)$ are defined as follows

$$A_{s7} = \frac{2}{(e^{gh_2}-e^{-gh_2})} \quad A_{s8} = \frac{(e^{-gh_2}+e^{gh_2})}{(e^{-gh_2}-e^{gh_2})} \quad A_{s9} = \frac{2(-e^{-gh_2}-e^{gh_2}+2)}{(e^{-gh_2}-e^{gh_2})} \tag{C.15}$$

Appendix D

The deflection and axial displacement solution for the laminated region ($L_1 < x < L_2$) in Eqs. (66) and (67) are derived as follows. Define the operator D as $D = d/dx$, then the mechanical governing equations in Eqs. (58) and (59) can be written as

$$(a_3D^4 + a_6D^6)w + (a_5D^5 + T_4D^4 + a_7D^3)u_0 = q \tag{D.1}$$

$$(a_2D^3 + T_{10}D^4 + a_8D^5)w + (a_4D^4 + a_1D^2)u_0 = 0 \tag{D.2}$$

According to the Eqs. (D.1) and (D.2), the following equation with only deflection parameter is derived as

$$(m_1D^4 + m_2D^3 + m_3D^2 + m_4D + m_5)D^6w = 0 \tag{D.3}$$

The solution $w(x)$ of Eq. (D.3) is written as

$$w = w_{s1} + w_{s2} \tag{D.4}$$

The deflection w_{s1} satisfies the following equation

$$D^6w_{s1} = 0 \tag{D.5}$$

Based on the reduction method, the deflection w_{s1} is derived as

$$w_{s1} = c_0 + c_1x + c_2x^2 + c_3x^3 + c_4x^4 + c_5x^5 \tag{D.6}$$

where $c_n(n = 1,2,3,4,5)$ are the constants to be determined. The deflection w_{s2} satisfies the following equation

$$(m_1D^4 + m_2D^3 + m_3D^2 + m_4D + m_5)w_{s2} = 0 \tag{D.7}$$

Let $w_{s2} = e^{rx}$, then the Eq. (D.7) becomes

$$m_1r^4 + m_2r^3 + m_3r^2 + m_4r + m_5 = 0 \tag{D.8}$$

The parameters $m_i(i=1,2,3,4,5)$ are already given in the Eq. (69). To solve the Eq. (D.8) conveniently, let $r = -\frac{m_2}{4m_1} + y$, then Eq. (D.8) is written as

$$y^4 + Py^2 + Qy + R = 0 \tag{D.9}$$

The parameters P, Q and R are also given in the Eq. (69). Define $y = A_1 + A_2 + A_3$, we obtain the cubic equation about the parameter A^2 as follows

$$A^6 + \frac{1}{2}PA^4 + \frac{1}{16}(P^2-4R)A^2 - \frac{1}{64}Q^2 = 0 \tag{D.10}$$

Let $A^2 = -\frac{1}{6}P + B$, we derive the cubic equation about the parameter B without quadratic term as follows

$$B^3 - \frac{P^2+12R}{48}B + \frac{72PR-27Q^2-2P^3}{1728} = 0 \tag{D.11}$$

To solve the Eq. (D.11) conveniently, let $B = C_1 + C_2$, then we obtain the quadratic equation about the parameter C^3 as follows

$$C^6 + \frac{72PR-27Q^2-2P^3}{1728}C^3 + (\frac{P^2+12R}{144})^3 = 0 \tag{D.12}$$

Based on the Eq. (D.12), we obtain the following equation

$$A^2 = -\frac{P}{6} + \sqrt[3]{m_7+\sqrt{m_8}} + \sqrt[3]{m_7-\sqrt{m_8}} \quad (if \quad m_8 \geq 0)$$
$$or$$
$$A^2 = -\frac{P}{6} + (\frac{1}{6}\sqrt{P^2+12R})cos(\frac{1}{3}arcsin(\sqrt{(1-m_7-\frac{m_8}{m_7})})) \quad (if \quad m_8 < 0) \tag{D.13}$$

The parameters $m_i(i=7,8)$ are given in the Eq. (69). Considering the relation $r = -\frac{m_2}{4m_1} + y$ and $y = A_1 + A_2 + A_3$, after some transformation and simplification, we obtain the following equations

$$r_1 = -\frac{m_2}{4m_1} + \sqrt{m_6} + \sqrt{-m_6 - \frac{P}{2} + 2\sqrt{m_6^2 + \frac{1}{2}Pm_6 + \frac{1}{16}(P^2-4R)}}$$
$$r_2 = -\frac{m_2}{4m_1} + \sqrt{m_6} - \sqrt{-m_6 - \frac{P}{2} + 2\sqrt{m_6^2 + \frac{1}{2}Pm_6 + \frac{1}{16}(P^2-4R)}}$$
$$r_3 = -\frac{m_2}{4m_1} - \sqrt{m_6} + \sqrt{-m_6 - \frac{P}{2} - 2\sqrt{m_6^2 + \frac{1}{2}Pm_6 + \frac{1}{16}(P^2-4R)}}$$
$$r_4 = -\frac{m_2}{4m_1} - \sqrt{m_6} - \sqrt{-m_6 - \frac{P}{2} - 2\sqrt{m_6^2 + \frac{1}{2}Pm_6 + \frac{1}{16}(P^2-4R)}}$$
$$(if \quad m_8 \geq 0) \tag{D.14}$$

Therefore, according to the Eqs. (D.7), (D.8) and (D.14), the deflection w_{s2} is written as

$$w_{s2} = c_6e^{r_1x} + c_7e^{r_2x} + c_8e^{r_3x} + c_9e^{r_4x} \tag{D.15}$$

where $c_n(n=6,7,8,9)$ are constants to be determined.

Based on the Eqs. (D.4), (D.6) and (D.15), the deflection $w(x)$ is written as

$$w(x) = c_0 + c_1x + c_2x^2 + c_3x^3 + c_4x^4 + c_5x^5 + c_6e^{r_1x} + c_7e^{r_2x} + c_8e^{r_3x} + c_9e^{r_4x} \tag{D.16}$$

Then, inserting Eq. (D.16) into Eq. (D.1), using the similar method, we can derive the axial displacement u_0 as

$$u_0 = c_{10} + c_{11}x + c_{12}x^2 + c_{14}e^{r_5x} + c_{15}e^{r_6x} - \frac{5a_3c_5}{a_7}x^4 + (\frac{q-24a_3c_4}{6a_7} - \frac{20T_6a_3c_5}{a_7^2})x^3 + \frac{(-a_3r_1^4 - a_6r_1^6)}{(-a_8r_1^5 + T_4r_1^4 + a_7r_1^3)}c_6e^{r_1x} + \frac{(-a_3r_2^4 - a_6r_2^6)}{(-a_8r_2^5 + T_4r_2^4 + a_7r_2^3)}c_7e^{r_2x} + \frac{(-a_3r_3^4 - a_6r_3^6)}{(-a_8r_3^5 + T_4r_3^4 + a_7r_3^3)}c_8e^{r_3x} + \frac{(-a_3r_4^4 - a_6r_4^6)}{(-a_8r_4^5 + T_4r_4^4 + a_7r_4^3)}c_9e^{r_4x} \tag{D.17}$$

with

$$r_5 = \frac{-T_4 + \sqrt{T_4^2 - 4a_5a_7}}{2a_5} \quad r_6 = \frac{-T_4 - \sqrt{T_4^2 - 4a_5a_7}}{2a_5} \tag{D.18}$$

According to the Eqs. (D.1), (D.2), (D.16) and (D.17), the relations among the undetermined constants $c_n(n=1,2,3,\ldots,15)$ are confirmed, thus the deflection and axial displacement solution for the mechanical governing equations in Eqs. (58) and (59) are determined and shown in Eqs. (66) and (67), respectively.

Appendix E

The unknown constants $b_n(n = 1, 2, 3, 4, 5)$ in the Eqs. (83) and (84) are determined as follows

$$b_{1f} = (\frac{2f_{3113}}{\alpha} - \frac{f_{3311}}{\alpha(1+\alpha\varepsilon_0)})w^{(2)} - \frac{f_{1113}(h_1+h_2)}{2\alpha(1+\alpha\varepsilon_0)}w^{(3)} + \frac{V}{\alpha h_2} - \frac{f_{1113}}{\alpha}u_0^{(2)} \tag{E.1}$$

$$b_{1p} = -\frac{d_{31}(h_1+h_2)}{2\alpha(1+\alpha\varepsilon_0)}w^{(2)} - \frac{d_{31}}{\alpha}u_0^{(1)} \tag{E.2}$$

$$b_{2f} = \frac{f_{1113}\varepsilon_0}{g(1+\alpha\varepsilon_0)}(1-e^{gh_2})A_s w^{(3)} + \frac{\frac{h_1}{2}f_{3311}g\varepsilon_0}{(1+\alpha\varepsilon_0)}e^{gh_2}A_s w^{(2)} - \frac{(h_2+\frac{h_1}{2})f_{3311}g\varepsilon_0}{(1+\alpha\varepsilon_0)}A_s w^{(2)} + \frac{f_{3311}g\varepsilon_0}{(1+\alpha\varepsilon_0)}(e^{gh_2}-1)A_s u_0^{(1)} \tag{E.3}$$

$$b_{2p} = \frac{d_{31}\varepsilon_0}{g(1+\alpha\varepsilon_0)}(1-e^{gh_2})A_s w^{(2)} \tag{E.4}$$

$$b_{3f} = \frac{f_{1113}\varepsilon_0}{g(1+\alpha\varepsilon_0)}(1-e^{-gh_2})B_s w^{(3)} + \frac{\frac{h_1}{2}f_{3311}g\varepsilon_0}{(1+\alpha\varepsilon_0)}e^{-gh_2}B_s w^{(2)} - \frac{(h_2+\frac{h_1}{2})f_{3311}g\varepsilon_0}{(1+\alpha\varepsilon_0)}B_s w^{(2)} + \frac{f_{3311}g\varepsilon_0}{(1+\alpha\varepsilon_0)}(e^{-gh_2}-1)B_s u_0^{(1)} \tag{E.5}$$

$$b_{3p} = \frac{d_{31}\varepsilon_0}{g(1+\alpha\varepsilon_0)}(1-e^{-gh_2})B_s w^{(2)} \tag{E.6}$$

$$b_{4f} = (\frac{f_{1113}b_{33}\varepsilon_0}{(1+\alpha\varepsilon_0)^2} + \frac{f_{1113}h_1(2h_2+h_1)}{8(1+\alpha\varepsilon_0)})w^{(3)} - \frac{f_{3311}}{(1+\alpha\varepsilon_0)}u_0^{(1)} - \frac{Vh_1}{2h_2} \tag{E.7}$$

$$b_{4p} = (\frac{d_{31}b_{33}\varepsilon_0}{(1+\alpha\varepsilon_0)^2} + \frac{d_{31}h_1(2h_2+h_1)}{8(1+\alpha\varepsilon_0)})w^{(2)} \tag{E.8}$$

$$b_{5f} = \frac{f_{3311}}{(1+\alpha\varepsilon_0)}w^{(2)} + \frac{f_{1113}(h_2+h_1)}{2(1+\alpha\varepsilon_0)}w^{(3)} - \frac{V}{h_2} \tag{E.9}$$

$$b_{5p} = \frac{d_{31}(h_2+h_1)}{2(1+\alpha\varepsilon_0)}w^{(2)} \tag{E.10}$$

The unknown constants $b_n(n = 1, 2, 3, 4, 5)$ are determined as

$$b_1 = b_{1f} + b_{1p} \quad b_2 = b_{2f} + b_{2p} \quad b_3 = b_{3f} + b_{3p} \quad b_4 = b_{4f} + b_{4p} \quad b_5 = b_{5f} + b_{5p} \tag{E.11}$$

Here, b_{if} and $b_{ip}(i = 1, 2, 3, 4, 5)$ are the coefficients associated with the flexoelectric effects and piezoelectric effects, respectively .

Appendix F

The deflection and axial displacement solution for the laminated region $(L_1 < x < L_2)$ in Eqs. (66) and (67) are derived as follows. Define the operator D as $D = d/dx$, then the mechanical governing equations in Eqs. (58) and (59) can be written as

$$T_{i1} = T_1 - \frac{2bf_{3113}^2h_2}{\alpha} + \frac{bf_{3113}f_{3311}h_2}{\alpha(1+\alpha\varepsilon_0)} + \frac{bd_{31}f_{3113}h_2(h_1+h_2)}{\alpha} - \frac{bd_{31}^2(h_1+h_2)^2h_2}{4\alpha(1+\alpha\varepsilon_0)} - \frac{bd_{31}f_{3311}\varepsilon_0h_2(h_1+h_2)}{2(1+\alpha\varepsilon_0)} \tag{F.1}$$

$$T_{i2} = T_2 + \frac{bf_{1113}^2h_2(h_1+h_2)^2}{4\alpha(1+\alpha\varepsilon_0)} \tag{F.2}$$

$$T_{i3} = \frac{bf_{1113}^2h_2(h_2+h_1)}{2\alpha} \tag{F.3}$$

$$T_{i4} = \frac{bf_{1113}f_{3311}h_2(1+2\alpha\varepsilon_0)}{\alpha(1+\alpha\varepsilon_0)} - \frac{bf_{1113}f_{3311}\varepsilon_0}{g(1+\alpha\varepsilon_0)}A_{s9} \tag{F.4}$$

$$T_{i5} = -\frac{1}{2}\frac{bgf_{3311}^2\varepsilon_0(h_2+h_1)}{(1+\alpha\varepsilon_0)}A_{s9} + \frac{bf_{3113}d_{31}h_2}{\alpha} - \frac{bd_{31}^2h_2(h_2+h_1)}{2\alpha} - \frac{bf_{3311}\varepsilon_0d_{31}}{g(1+\alpha\varepsilon_0)}A_{s9} \tag{F.5}$$

$$T_{i6} = (-\frac{1}{2}\frac{bf_{3311}f_{1113}\varepsilon_0(h_2+h_1)}{g(1+\alpha\varepsilon_0)} + \frac{bd_{31}f_{1113}\varepsilon_0}{g^3(1+\alpha\varepsilon_0)})A_{s9} - \frac{bd_{31}f_{1113}h_2\varepsilon_0}{g^2(1+\alpha\varepsilon_0)} + \frac{bd_{31}f_{1113}\varepsilon_0}{(1+\alpha\varepsilon_0)}[\frac{-h_1^3}{24} + \frac{(h_2+\frac{1}{2}h_1)^3}{3}] \tag{F.6}$$

$$T_{i7} = T_7 \tag{F.7}$$

$$T_{i8} = T_8 + \frac{2bd_{31}f_{3311}\varepsilon_0h_2}{(1+\alpha\varepsilon_0)} - \frac{2bd_{31}f_{3113}h_2}{\alpha} + \frac{bd_{31}f_{3311}h_2}{\alpha(1+\alpha\varepsilon_0)} + \frac{bd_{31}^2h_2(h_1+h_2)}{2\alpha(1+\alpha\varepsilon_0)} \tag{F.8}$$

$$T_{i9} = -\frac{bf_{1113}d_{31}h_2(h_2+h_1)}{2\alpha} \tag{F.9}$$

$$T_{i10} = \frac{2bf_{1113}f_{3113}h_2}{\alpha} - \frac{bf_{3311}f_{1113}h_2}{\alpha(1+\alpha\varepsilon_0)} - \frac{bf_{1113}f_{3311}\varepsilon_0}{g(1+\alpha\varepsilon_0)}A_{s9} \tag{F.10}$$

$$T_{i11} = -\frac{bf_{1113}^2h_2}{\alpha} \tag{F.11}$$

$$T_{i12} = \frac{bgf_{3311}^2\varepsilon_0}{(1+\alpha\varepsilon_0)}A_{s9} + \frac{bd_{31}^2h_2}{\alpha} \tag{F.12}$$

$$T_{i13} = -\frac{bf_{3311}f_{1113}\varepsilon_0h_2}{(1+\alpha\varepsilon_0)} - \frac{bd_{31}f_{1113}\varepsilon_0h_2(h_2+h_1)}{2(1+\alpha\varepsilon_0)} + \frac{2bf_{3113}f_{1113}h_2}{\alpha} - \frac{bf_{3311}f_{1113}h_2}{\alpha(1+\alpha\varepsilon_0)} - \frac{bf_{1113}d_{31}h_2(h_2+h_1)}{2\alpha(1+\alpha\varepsilon_0)} \tag{F.13}$$

$$T_{i14} = -\frac{bd_{31}f_{1113}h_2}{\alpha} \tag{F.14}$$

References

[1] Zubko P, Catalan G, Buckley A, Welche PRL, Scott JF. Strain-gradient-induced polarization in $SrTiO_3$ single crystals. Phys Rev Lett 2007;99(16):167601.

[2] Shu L, Ke S, Fei L, Huang W, Wang Z, Gong J, et al. Photoflexoelectric effect in halide perovskites. Nature Mater 2020;19(6):605–9.

[3] Yudin PV, Tagantsev AK. Fundamentals of flexoelectricity in solids. Nanotechnology 2013;24(43):432001.

[4] Toupin RA. The elastic dielectric. J Ration Mech Anal 1956;5(6):849–915.

[5] Wang GF, Yu SW, Feng XQ. A piezoelectric constitutive theory with rotation gradient effects. Eur J Mech A Solids 2004;23(3):455–66.

[6] Toupin R. Elastic materials with couple-stresses. Arch Ration Mech Anal 1962;11(1):385–414.

[7] Mindlin RD, Tiersten HF. Effects of couple-stresses in linear elasticity. Arch Ration Mech Anal 1962;11(1):415–48.

[8] Yang FACM, Chong ACM, Lam DCC, Tong P. Couple stress based strain gradient theory for elasticity. Int J Solids Struct 2002;39(10):2731–43.

[9] Hadjesfandiari AR, Dargush GF. Couple stress theory for solids. Int J Solids Struct 2011;48(18):2496–510.

[10] Li YS, Xiao T. Free vibration of the one-dimensional piezoelectric quasicrystal microbeams based on modified couple stress theory. Appl Math Model 2021;96:733–50.

[11] Hadjesfandiari AR. Size-dependent piezoelectricity. Int J Solids Struct 2013;50(18):2781–91.

[12] Münch I, Neff P, Madeo A, Ghiba ID. The modified indeterminate couple stress model: Why Yang, other's, arguments motivating a symmetric couple stress tensor contain a gap and why the couple stress tensor may be chosen symmetric nevertheless. ZAMM-J Appl Math Mech/Z Angew Math Mech 2017;97(12):1524–54.

[13] Neff P, Münch I, Ghiba ID, Madeo A. On some fundamental misunderstandings in the indeterminate couple stress model, a comment on recent papers of AR Hadjesfandiari and GF Dargush. Int J Solids Struct 2016;81:233–43.

[14] Shaat M. Physical and mathematical representations of couple stress effects on micro/nanosolids. Int J Appl Mech 2015;7(01):1550012.

[15] Fu G, Zhou S, Qi L. On the strain gradient elasticity theory for isotropic materials. Internat J Engrg Sci 2020;154(2020):1–25.

[16] Mindlin RD. Micro-structure in linear elasticity. Arch Ration Mech Anal 1964;16(1):51–78.

[17] Mindlin RD, Eshel NN. On first strain-gradient theories in linear elasticity. Int J Solids Struct 1968;4(1):109–24.

[18] Lam DC, Yang F, Chong ACM, Wang J, Tong P. Experiments and theory in strain gradient elasticity. J Mech Phys Solids 2003;51(8):1477–508.

[19] Li YS, Feng WJ, Cai ZY. Bending and free vibration of functionally graded piezoelectric beam based on modified strain gradient theory. Compos Struct 2014;115:41–50.

[20] Zhou S, Li A, Wang B. A reformulation of constitutive relations in the strain gradient elasticity theory for isotropic materials. Int J Solids Struct 2016;2:8–37.
[21] Aifantis EC. On the role of gradients in the localization of deformation and fracture. Internat J Engrg Sci 1992;30(10):1279–99.
[22] Aravas N. Plane-strain problems for a class of gradient elasticity modelsa stress function approach. J Elasticity 2011;104(1):45–70.
[23] Yue YM, Xu KY, Aifantis EC. Microscale size effects on the electromechanical coupling in piezoelectric material for anti-plane problem. Smart Mater Struct 2014;23(12):125043.
[24] Fleck NA, Hutchinson J. A reformulation of strain gradient plasticity. J Mech Phys Solids 2001;49(10):2245–71.
[25] Fu G, Zhou S, Qi L. A size-dependent Bernoulli–Euler beam model based on strain gradient elasticity theory incorporating surface effects. ZAMM-J Appl Math Mech/Z Angew Math Mech 2019;99(6):e201800048.
[26] Mindlin RD. Polarization gradient in elastic dielectrics. Int J Solids Struct 1968;4(6):637–42.
[27] Tagantsev AK. Piezoelectricity and flexoelectricity in crystalline dielectrics. Phys Rev B 1986;34(8):5883.
[28] Yan Z, Jiang L. Size-dependent bending and vibration behaviour of piezoelectric nanobeams due to flexoelectricity. J Phys D: Appl Phys 2013;46(35):355502.
[29] Guo Y, Huang B, Wang J. Thickness-stretch vibration of an infinite piezoelectric plate with flexoelectricity. Appl Sci 2022;12(5):2436.
[30] Barati MR. On non-linear vibrations of flexoelectric nanobeams. Internat J Engrg Sci 2017;121:143–53.
[31] Majdoub MS, Sharma P, Cagin T. Enhanced size-dependent piezoelectricity and elasticity in nanostructures due to the flexoelectric effect. Phys Rev B 2008;77(12):125424.
[32] Sahin E, Dost S. A strain-gradients theory of elastic dielectrics with spatial dispersion. Internat J Engrg Sci 1988;26(12):1231–45.
[33] Li A, Zhou S, Qi L, Chen X. A reformulated flexoelectric theory for isotropic dielectrics. J Phys D: Appl Phys 2015;48(46):465502.
[34] Awad E, El Dhaba AR, Fayik M. A unified model for the dynamical flexoelectric effect in isotropic dielectric materials. Eur J Mech-A/Solids 2022;104618.
[35] Enakoutsa K, Corte AD, Giorgio I. A model for elastic flexoelectric materials including strain gradient effects. Math Mech Solids 2016;21(2):242–54.
[36] Baroudi S, Najar F, Jemai A. Static and dynamic analytical coupled field analysis of piezoelectric flexoelectric nanobeams: A strain gradient theory approach. Int J Solids Struct 2018;135:110–24.
[37] Li X, Luo Y. Flexoelectric effect on vibration of piezoelectric microbeams based on a modified couple stress theory. Shock Vib 2017;2017.
[38] Wang KF, Wang BL. An analytical model for nanoscale unimorph piezoelectric energy harvesters with flexoelectric effect. Compos Struct 2016;153:253–61.
[39] Hu S, Shen S. Variational principles and governing equations in nano-dielectrics with the flexoelectric effect. Sci China Phys Mech Astron 2010;53(8):1497–504.
[40] Shen S, Hu S. A theory of flexoelectricity with surface effect for elastic dielectrics. J Mech Phys Solids 2010;58(5):665–77.
[41] Zhang J, Li XF. Bending of piezoelectric beams with the flexoelectric effect under applied load at any position. Modern Phys Lett B 2018;32(30):1850372.0372.
[42] Zhou ZD, Yang CP, Su YX, Huang R, Lin XL. Electromechanical coupling in piezoelectric nanobeams due to the flexoelectric effect. Smart Mater Struct 2017;26(9):095025.
[43] Chen Y, Zhang M, Su Y, Zhou Z. Coupling analysis of flexoelectric effect on functionally graded piezoelectric cantilever nanobeams. Micromachines 2021;12(6):595.
[44] Su YX, Zhou ZD, Yang FP. Electromechanical analysis of bilayer piezoelectric sensors due to flexoelectricity and strain gradient elasticity. AIP Adv 2019;9(1):015207.
[45] Fu G, Zhou S, Qi L. On the size dependency of a dielectric partially covered laminated microbeam. Thin-Walled Struct 2021;161:107489.
[46] Chen W, Liang X, Shen S. Forced vibration of piezoelectric and flexoelectric Euler–Bernoulli beams by dynamic Green's functions. Acta Mech 2021;232(2):449–60.
[47] Sondipon A. Flexoelectric effect on vibration responses of piezoelectric nanobeams embedded in viscoelastic medium based on nonlocal elasticity theory. Acta Mech 2018;229(6):2379.
[48] Malikan M, Eremeyev VA. On the dynamics of a viscopiezoflexoelectric nanobeam. Symmetry 2020;12(4):643.
[49] Wang KF, Wang BL, Zeng S. Analysis of an array of flexoelectric layered nanobeams for vibration energy harvesting. Compos Struct 2018;187:48–57.
[50] Wang KF, Wang BL. Non-linear flexoelectricity in energy harvesting. Internat J Engrg Sci 2017;116:88–103.
[51] Liang X, Zhang R, Hu S, Shen S. Flexoelectric energy harvesters based on timoshenko laminated beam theory. J Intell Mater Syst Struct 2017;28(15):2064–73.
[52] Tadi Beni Y. Size-dependent electromechanical bending, buckling, and free vibration analysis of functionally graded piezoelectric nanobeams. J Intell Mater Syst Struct 2016;27(16):2199–215.
[53] Ghobadi A, Beni YT, Golestanian H. Size dependent thermo-electro-mechanical nonlinear bending analysis of flexoelectric nano-plate in the presence of magnetic field. Int J Mech Sci 2019;152:118–37.
[54] Jankowski P, ur KK, Kim J, Lim CW, Reddy JN. On the piezoelectric effect on stability of symmetric FGM porous nanobeams. Compos Struct 2021;267:113880.
[55] Mawassy N, Reda H, Ganghoffer JF, Eremeyev VA, Lakiss H. A variational approach of homogenization of piezoelectric composites towards piezoelectric and flexoelectric effective media. Internat J Engrg Sci 2021;158:103410.
[56] Yan Z. Size-dependent bending and vibration behaviors of piezoelectric circular nanoplates. Smart Mater Struct 2016;25(3):035017.
[57] He L, Lou J, Zhang A, Wu H, Du J, Wang J. On the coupling effects of piezoelectricity and flexoelectricity in piezoelectric nanostructures. AIP Adv 2017;7(10):105106.
[58] Zhang Z, Yan Z, Jiang L. Flexoelectric effect on the electroelastic responses and vibrational behaviors of a piezoelectric nanoplate. J Appl Phys 2014;116(1):014307.
[59] Yan Z. Size-dependent bending and vibration behaviors of piezoelectric circular nanoplates. Smart Mater Struct 2016;25(3):035017.
[60] Wang KF, Wang BL. Energy gathering performance of micro/nanoscale circular energy harvesters based on flexoelectric effect. Energy 2018;149:597–606.
[61] Guinovart-Sanjuán D, Vajravelu K, Rodríguez-Ramos R, Guinovart-Díaz R, Sabina FJ, Merodio J. Simple closed-form expressions for the effective properties of multilaminated flexoelectric composites. J Eng Math 2021;127:1–13.
[62] Guinovart-Sanjuán D, Vajravelu K, Rodríguez-Ramos R, Guinovart-Díaz R, Bravo-Castillero J, Lebon F, et al. Effective predictions of heterogeneous flexoelectric multilayered composite with generalized periodicity. Int J Mech Sci 2020;181:105755.
[63] Serpilli M, Rizzoni R, Rodríguez-Ramos R, Lebon F, Dumont S. A novel form of imperfect contact laws in flexoelectricity. Compos Struct 2022;300:116059.
[64] Jiang X, Huang W, Zhang S. Flexoelectric nano-generator: Materials, structures and devices. Nano Energy 2013;2(6):1079–92.
[65] Wang KF, Wang BL, Kitamura T. A review on the application of modified continuum models in modelling and simulation of nanostructures. Acta Mech Sinica 2016;32(1):83–100.
[66] Chen Q, Zheng S, Li Z, Zeng C. Size-dependent free vibration analysis of functionally graded porous piezoelectric sandwich nanobeam reinforced with graphene platelets with consideration of flexoelectric effect. Smart Mater Struct 2021;30(3):035008.
[67] Mao S, Purohit PK. Insights into flexoelectric solids from strain-gradient elasticity. J Appl Mech 2014;81(8).
[68] Fu G, Zhou S, Qi L. The size-dependent static bending of a partially covered laminated microbeam. Int J Mech Sci 2019;152:411–9.